

Coupled Geothermal Power and Direct Air Capture with Storage

Prepared for:

United States Energy Association (USEA) in Cooperation with the U.S. Department of Energy
– Office of Fossil Energy under Subagreement 633-2024-004-03



Prepared by:

Battelle Memorial Institute



September 24, 2024

Subagreement No. 633-2024-004-03

Coupled Geothermal Power and Direct Air Capture with Storage

Prepared by:

Battelle
505 King Avenue
Columbus, Ohio 43201

Submitted to:

United States Energy Association

Technical Point of Contact:

Neeraj Gupta
Senior Research Leader
Battelle, Columbus, OH
Email: gupta@battelle.org
Phone: 614-424-3820

Contractual Point of Contact:

Lauren Newkirk
Contracts Specialist
Battelle, Columbus, OH
Email: newkirk@battelle.org
Phone: 614-424-5071

Technical Point of Contact:

Amy Lang
Project Manager
Battelle, Columbus, OH
Email: lang@battelle.org
Phone: 614-424-6131

September 24, 2024

Subagreement No. 633-2024-004-03

Coupled Geothermal Power and Direct Air Capture with Storage

Prepared by:

Aubrey Collie, Abby Dietrich, Ryan Adams, Abigail Goehring, Brigitte Petras, and Jorge Barrios Rivas

Battelle

505 King Avenue

Columbus, Ohio 43201

Submitted to:

United States Energy Association

This report was prepared by Battelle as an account of work sponsored by United States Energy Association (USEA) in cooperation with the U.S. Department of Energy (DOE). Neither the United States Government, nor any agency thereof, nor any of their employees, nor Battelle and other cosponsors, makes any warranty, express or implied, or assumes any liability or responsibility for the accuracy, completeness, or usefulness of any information, apparatus, product, or process disclosed, or represents that its use would not infringe privately owned rights. Reference herein to any specific commercial product, process, or service by trade name, trademark, manufacturer, or otherwise does not necessarily constitute or imply its endorsement, recommendations, or favoring by the United States Government or any agency thereof. The views and the opinions of authors expressed herein do not necessarily state or reflect those of the United States Government or any agency thereof.

Battelle does not engage in research for advertising, sales promotion, or endorsement of our clients' interests including raising investment capital or recommending investments decisions, or other publicity purposes, or for any use in litigation.

Battelle endeavors at all times to produce work of the highest quality, consistent with our contract commitments. However, because of the research and/or experimental nature of this work the client undertakes the sole responsibility for the consequence of any use or misuse of, or inability to use, any information, apparatus, process or result obtained from Battelle, and Battelle, its employees, officers, or Trustees have no legal liability for the accuracy, adequacy, or efficacy thereof.

Executive Summary

The Intergovernmental Panel on Climate Change (IPCC) estimates that to avoid the direst consequences of climate change, the world must implement millions or even billions of tons of atmospheric carbon dioxide removal (CDR) by 2100. Direct air capture (DAC) is one method to accomplish CDR, but is an energy intensive process, requiring high heat for carbon dioxide (CO₂) desorption. Powering DAC with geothermal energy may be an option, as it provides consistent, predictable, low-carbon energy that wind and solar cannot due to their reliance on day-to-day environmental conditions and diurnal fluctuation. Some high-quality geothermal play fairways are likely to be located near or even in suitable carbon storage fairways. This study identifies current and prospective geothermal energy production fairways, current and prospective carbon storage fairways, and highlights where the two fairway types are closely coupled. In order to identify which geographic regions are most suitable for geothermally powered direct air capture and storage (GDACS), the currently available DAC technologies and their power needs have been assessed as well as the potential power output and storage capacities of geothermal fairways and storage fairways, respectively, and these assessments have been integrated into a model that predicts performance and cost per stored tonne of CO₂ for a conceptual GDACS facility located in each fairway.

Table of Contents

	Page
Coupled Geothermal Power and Direct Air Capture with Storage.....	2
Draft Report Error! Bookmark not defined.	
Disclaimer Error! Bookmark not defined.	
Executive Summary	i
1.0 Introduction and Problem Statement.....	1
2.0 Fundamentals of a Three-Part System	3
2.1 Fundamentals of Geothermal Systems.....	3
2.1.1 Key Components of Geothermal Systems	3
2.1.2 Types of Geothermal Systems.....	4
2.1.3 Temperature/Depth Ranges	7
2.1.4 Geologic Settings	9
2.1.5 Distribution of Geothermal Resources in the US.....	11
2.1.6 Factors Influencing Cost of Geothermal Power.....	12
2.1.7 Geothermal Power Plants.....	14
2.2 Fundamentals of CO ₂ Geologic Storage.....	15
2.2.1 Geologic Settings	15
2.2.2 Temperature and Depth Ranges for Geological Carbon Storage.....	17
2.2.3 Play Types.....	19
2.2.4 Geographic Locations of Carbon Storage Fairways.....	20
2.2.5 Range of Geological Carbon Storage Potentials.....	21
2.2.6 Estimated Cost per Tonne of Stored CO ₂	23
2.3 Fundamentals of DAC systems	24
2.3.1 Range of DAC Technologies	24
2.3.2 Range of DAC Operating Temperatures	27
2.3.3 Impact of Local Climate on DAC Operations.....	28
2.3.4 Energy Consumption Range (GJ/tCO ₂)	28
2.3.5 Estimated Cost per Tonne for DAC Systems	29
3.0 Capacity & Cost Modeling: Powering DACS with Geothermal Energy	30
3.1 Model Setup	30
3.2 Assumptions.....	30
3.3 Geothermal Energy	31
3.3.1 Assumptions.....	31

- 4.3.2 Model Recommendations 31
- 3.4 Direct Air Capture Facility 31
 - 3.4.1 Model Recommendations 34
- 3.5 Transportation 34
 - 3.5.1 Transportation Calculations 34
 - 3.5.2 Assumptions 35
 - 3.5.3 Model Recommendations 35
- 3.6 Geological Storage 35
 - 3.6.1 Storage Calculations 35
 - 3.6.2 Assumptions 35
- 4.0 Uncertainties and Recommendations for Future Work 37
 - 4.1 Uncertainties in geothermal energy development 37
 - 4.2 Uncertainties in carbon storage development 37
 - 4.3 Uncertainties in DAC development 37
 - 4.4 Uncertainties in GDACS development 38
 - 4.5. Uncertainties in the GDACS Cost and Capacity Model 38
 - 4.5.1 Global model uncertainties 38
 - 4.5.2. DAC model uncertainties 38
 - 4.5.3 Transportation model uncertainties 40
 - 4.5.4 Storage model uncertainties 40
 - 4.6 Recommendations for Future Models: 41
 - 4.6.1. Global Recommendations 41
 - 4.6.2. Geothermal Power Model Recommendations 41
 - 4.6.3. DAC Model Recommendations 42
 - 4.6.4. Transportation Model Recommendations 43
 - 4.6.5. Storage Model Recommendations 43
- 5.0 References 45
- Acknowledgements 53

List of Figures

	Page
Figure 1-1: Geothermal energy (red line) compared to other sources of renewable energy. Note the consistent power output of geothermal energy versus the strong diurnal signal of solar (yellow line) and the inconsistent signal of meteorologically controlled wind power (blue line). Source: Think Geoenergy, graph from California Independent System Operator (CAISO).....	2

Figure 2-1: Example of key components of enhanced geothermal systems (Source: Rizzi, 2023). 4

Figure 2-2: Geothermal technology overview across conventional hydrothermal systems (left) and next-generation designs (right). (Source: Blankenship et al., 2024). 7

Figure 2-3: Common energy applications based on geothermal temperature ranges (Source: Rizzi, 2023). 8

Figure 2-4: Global view of plate tectonic boundary-associated geothermal fields. Note predominance of fields along the west coast of the U.S. (Source: Moeck, 2014). 10

Figure 2-5: Number of geothermal power plants in the United States as of 2021, by state (Fernández, 2024). 12

Figure 2-6: Levelized cost of energy comparison—unsubsidized analysis (Source: Lazard, 2023). 13

Figure 2-7: Future cost reduction, modified from Blankenship (2024). 14

Figure 2-8: 2023 Historical LCOE by NREL annual technology baseline. 14

Figure 2-9: Example of Static Earth Modeling using subsurface data (Source: Ajayi, 2019). 17

Figure 2-10: Graph showing relationship between CO₂ density and subsurface depth. As depth increases, so does density, making deeper storage reservoirs generally preferable to shallow reservoirs. (Source: National Energy Technology Laboratory, 2024). 18

Figure 2-11: Options for geological storage of CO₂ (Benson, 2016). 19

Figure 2-12: US Regional Carbon Sequestration Partnership areas (NETL, 2015). 21

Figure 2-13: P5-P95 estimates of carbon storage potential for key basins within the United States. Basins at the top of the graph have relatively low storage capacities, while basins at the bottom of the graph have large capacities. Basins of note include the U.S. Gulf Coast Basin with over 1,000 billion metric tons of accessible storage, the Illinois and Michigan basins in the Midwest, the Williston and Thrust Belt basins in the Rockies regions, and the Appalachian Basin in the eastern U.S. (modified from USGS, 2013). 22

Figure 2-14: Estimated range of CO₂ capture costs (Data source: Congressional Budget Office, 2023). 23

Figure 2-15: Indicative unit CO₂ pipeline transport costs (IEA, 2020). 24

Figure 2-16: Typical alkali-scrubbing liquid DAC process (Sabatino et al., 2021). 25

Figure 2-17: Typical amine-scrubbing liquid DAC process (Sabatino et al., 2021). 25

Figure 2-18: Example of a solid sorbent DAC system (Sabatino et al., 2021). 26

Figure 2-19: VTSA cycle schematic shown as four steps to capture CO₂ from ambient air and regenerate the sorbent (Sabatino et al., 2021). 27

Figure 2-20: DAC technology, ranked as high temperature (HT) or low temperature (LT), used by companies and their CO₂ regeneration temperatures (Sabatino et al., 2021). 27

Figure 2-21: Energy requirement per ton CO₂ captured (IEA, 2023). 28

Figure 2-22: Pipeline transportation costs based on distances for regions in the U.S. using two different models: Parker (2004) and McCoy and Rubin (2008) (Stolaroff et al., 2021). 29

List of Tables

Table 2-1: Geothermal Resource and Cost Characteristics (Source: National Renewable Energy Laboratory, 2023). 14

List of Attachments

Example Play Fairways: Geothermally-powered Direct Air Capture + Storage

Coupled Geothermal Power and Direct Air Capture with Storage: Fairway Maps, Contiguous United States

1.0 Introduction and Problem Statement

The Intergovernmental Panel on Climate Change (IPCC) estimates that to avoid the most disruptive consequences of climate change, the world must implement millions or even billions of tons of atmospheric carbon dioxide removal (CDR) by 2100 (IPCC, 2022). CDR is required first because total emissions are expected to exceed the target necessary to limit global warming to 2°C or less, and because, even if emissions reductions were to progress rapidly, hard-to-abate emissions from industries, such as steel and cement production, will likely need to be mitigated via CDR to reach a true 'net zero emissions' economy.

Multiple pathways exist to implement CDR and fall into two basic categories:

1. Nature-based solutions, which include afforestation, reforestation, soil carbon sequestration, ocean fertilization, and other agricultural or bioculture-based solution, and
2. Engineered solutions, including enhanced rock weathering, bioenergy with carbon capture and storage (BECCS), and direct air carbon capture and storage (DACCS).

Nature-based CDR solutions are favorable because they tend to have relatively low upfront costs (for example, afforestation and reforestation may, in some cases, have a \$0 cost per tonne of CO₂ removed from the atmosphere) and may have co-benefits that complement their CO₂ removal potential (afforestation may result in improved or additional habitat for protected species; soil carbon sequestration may, in some cases, improve soil quality and crop yields). However, nature-based solutions come with drawbacks, such as competition for land resources, relatively short storage timescales (tens to hundreds of years) and difficulty measuring and verifying the scale of CO₂ removal from the atmosphere (IPCC, 2022).

Direct air capture (DAC) comprises a set of techniques and technologies used to capture CO₂ from the atmosphere via chemical reactions, strip the CO₂ from the sorbent or solvent material, and then send the CO₂ to be either stored geologically or used in industrial processes such as materials manufacturing or fuel production. DAC suffers from drawbacks, such as high energy intensity and high-cost relative to nature-based solutions. Additionally, some DAC technologies require process water usage, making these technologies unfavorable in water-challenged environments. However, DAC requires significantly less land use than other CDR methods and because it is an engineered solution, measurement and verification of CO₂ removal is relatively simple. DAC plus storage also provides the most durable CDR, with storage timescales measured in tens of thousands to millions of years (IPCC, 2022).

No single CDR solution is likely to be sufficient to complete all necessary CO₂ removal from the atmosphere. Therefore, DAC is likely to play an important role as a space-efficient engineered solution for CDR over the next several decades. In order to maintain the carbon-negative status of this technology, it will be necessary to power it using low-carbon energy. Most low-carbon energy sources suffer from intermittency, either due to meteorological events, in the case of wind power, or due to both meteorological and diurnal fluctuations, in the case of solar power (Shi et al., 2020). Geothermal energy, on the other hand, tends to provide relatively consistent power output, making it ideal for powering continuous industrial processes such as DAC (Figure 1-1, Think Geoenergy).

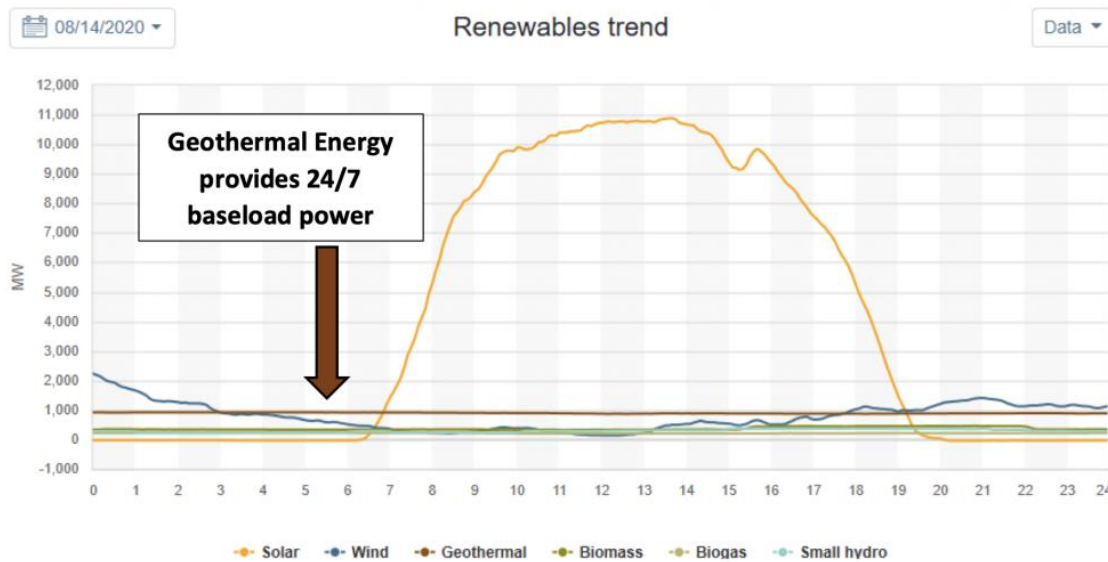


Figure 1-1: Geothermal energy (red line) compared to other sources of renewable energy. Note the consistent power output of geothermal energy versus the strong diurnal signal of solar (yellow line) and the inconsistent signal of meteorologically controlled wind power (blue line). Source: Think Geoenergy, graph from California Independent System Operator (CAISO).

In addition to geothermal energy's consistent output, it provides its power via heat derived from the earth. DAC technologies tend to require relatively high heat in some parts of the process (as described in detail in Section 2), so utilizing geothermal power for DAC may provide the co-benefit of being able to use residual heat remaining after the geothermal facility's power cycle to provide process heat, improving the energy efficiency of both the geothermal installation and the DAC process. The case for powering DAC facilities with geothermal energy is strong.

Once DAC is implemented, it is necessary to either use or dispose of the resultant CO₂. Currently, CO₂ utilization is nascent and is likely to represent a small percentage of the carbon capture, utilization, and storage (CCUS) market. Thus, most captured CO₂ is likely to be stored in geological storage. Because high-temperature geothermal resources tend to come from igneous and metamorphic geological terrains, not all geothermal energy developments are located within reasonable distance of a potential carbon storage reservoir.

The goal of this study is to gain an understanding of the relationship between the geology of geothermal plays and the geology of carbon storage plays, in order to highlight regions within the continental United States where geothermal direct air capture and storage (GDACS) facilities may be placed, and to estimate the storage potential of GDACS systems.

2.0 Fundamentals of a Three-Part System

2.1 Fundamentals of Geothermal Systems

Geothermal energy is a renewable energy source derived from the Earth's internal heat. The Earth's interior is hot because of three primary processes:

1. Heat derived from the accretion of the planet about 4.5 billion years ago and the Late Heavy Bombardment 4.0 to 3.8 billion years ago (Zhang, 2002)
2. Heat due to friction, which is caused by heavy crustal material sinking into the mantle, as well as movement of material within the core (Backus, 1975), and
3. Heating due to ongoing decay of radioactive isotopes within the Earth's core, mantle, and crust, such as uranium and potassium (Gupta & Roy, 2007).

Geothermal systems utilize this natural heat reservoir for electricity generation, building heating, and direct use of hot water for various applications (Tester et al., 2006).

2.1.1 Key Components of Geothermal Systems

Although there are multiple types of geothermal systems in the subsurface, the exploitation of geothermal energy systems relies on several key components. Figure 2-1 provides a basic overview of these components, which are summarized below.

1. Heat Source

Geothermal systems rely on the Earth's mantle and crust, which harbor significant heat reservoirs originating from the processes described in Section 2.1. Rocks have relatively low thermal conductivity (Abdulagatov et al., 2006), so shallow rocks act as an insulating blanket, causing heat to be stored deep in the subsurface where it can be accessed via drilling.

2. Reservoir

Geothermal reservoirs are underground zones where hot water or steam gathers. These reservoirs may be situated in fractured rock formations or permeable sedimentary layers. The reservoir's ability to store and transmit heat depends on factors like permeability and porosity.

3. Fluid Circulation System

Geothermal fluids, usually water or steam, flow through the reservoir and ascend to the surface via wells. This circulation mechanism facilitates the transfer of heat from the reservoir to the surface, where it can be harnessed for various applications. In some systems, where the supply of subsurface water is limited, water is added to the geothermal system from a surface source, heated by the hot rock, and then circulated to the surface for energy extraction.

4. Surface Power Plant

Upon reaching the surface, geothermal fluids are directed to power plants equipped with turbines and generators. The high-pressure steam or hot water extracted from the reservoir drives turbines, leading to the generation of electricity.

5. Heat Exchangers

In direct-use geothermal applications, heat exchangers are used to transfer heat from geothermal fluids to a secondary medium, such as water or air, for heating purposes in buildings or industrial processes.

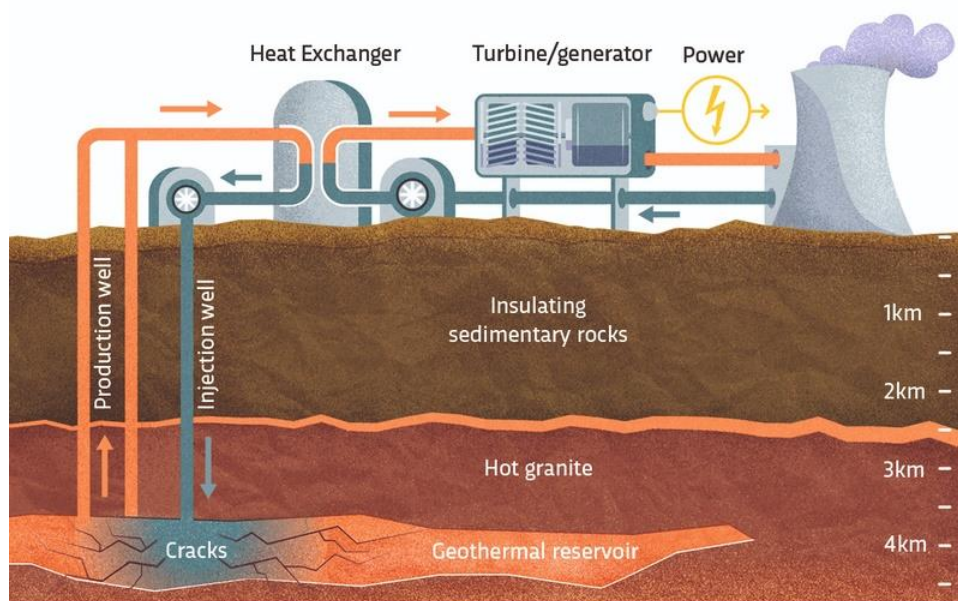


Figure 2-1: Example of key components of enhanced geothermal systems (Source: Rizzi, 2023).

2.1.2 Types of Geothermal Systems

Understanding the diverse range of geothermal systems is crucial for maximizing the utilization of this sustainable energy source. This overview presents key insights into various types of geothermal systems (Figure 2-2), key geological settings and geographic regions, and costs to develop geothermal energy.

1. Vapor-phase Hydrothermal Systems

Hydrothermal systems are usually found near tectonic plate boundaries, active volcanic zones, and areas with recent volcanism. Geological activities, such as volcanic processes and circulation of hydrothermal fluid associated with magma bodies, create these reservoirs, with surface signs such as lava flows, hot springs, geysers, and fumaroles, as well as subsurface reservoirs hosted in fractured or porous rock formations. Temperatures in these systems are in excess of 200°C, with power production accomplished by producing the geothermal fluids, which flash to steam as they rise up the wellbore or are flashed to steam within the power plant. The steam is then used to drive a turbine, producing electricity. Single well capacities may be up to 25 megawatts (MW) (Gupta & Roy, 2007; Moya et al., 2018; Khodayar & Bjornsson, 2024).

- Pros: Very high heat and resource density when available, established technology for drilling and production, proven viability for power generation.
- Cons: Limited geographical availability, high upfront exploration costs.

- Continental U.S. Fairway Locations: California and Nevada, with potential in the Basin and Range tectonic province and the Cascades ranges (currently producing at The Geysers in California).

2. Liquid-phase Hydrothermal Systems

Liquid-phase hydrothermal systems are characterized by the presence of natural hot water reservoirs in fractured, permeable rock formations. These systems occur in volcanically or tectonically active regions, and have reservoir temperatures between 100 and 200°C, insufficient to provide flash steam production. These systems provide electricity by utilizing a binary-cycle power plant, which transfers heat from water to a fluid with a lower boiling point, which is then flashed to vapor in order to run a turbine and generate electricity. Single well capacities may be up to 7 MW (Gupta & Roy, 2007; Tomarov & Shipkov, 2017; Khodayar & Bjornsson, 2024).

- Pros: Broader fairways than vapor-phase hydrothermal, lower-temperature drilling environment.
- Cons: Limited resource density, potentially challenging economics.
- Continental U.S. Fairway Locations: California, Nevada, Idaho, New Mexico, Colorado, with potential in the Basin and Range tectonic province, Cascades ranges, Rio Grande Rift System, central Rocky Mountains

3. Enhanced Geothermal Systems (EGS)

These systems, also referred to as ‘hot, dry rock’ systems, occur where a high-temperature geothermal system (generally temperatures greater than 200°C) is available, but the thermal reservoir lacks sufficient porosity and/or permeability to deliver geothermal fluids to a wellbore. In order to enhance the flow of these reservoirs, engineering techniques, such as hydraulic stimulation, are used to enhance existing fractures or create artificial fractures within the reservoir and then provide heat transfer by introducing water to the reservoir. Per-well power output varies widely (Fervo, personal communications).

- Pros: Potential for widespread deployment, not limited by natural flow, technical and economic limits not yet reached.
- Cons: Technological challenges, potential for induced seismicity, high upfront costs, water supply risk in arid regions.
- Continental U.S. Fairway Locations: Western US, consistent with high-temperature hydrothermal fairways. Current operations are limited, but research and production facilities are in operation in southwestern Utah and in development elsewhere in the Western US. Expansion of fairways is likely as technological advancements bring lower-temperature resources into economic viability (Fervo, personal communication).

4. Closed-loop Systems

Closed-loop systems, also known as advanced geothermal systems, function without fluid exchange between the well and the geothermal reservoir, eliminating the need for hydraulic fracturing. These systems involve drilling a single well into the heated formation and utilizing a concentric pipe-in-pipe setup to circulate fluids within the well, picking up heat from the reservoir and bringing it to the surface. Power output per well is highly variable, as these systems may be utilized at a broad range of depths and geothermal gradients (Van Horn et al., 2020).

- Pros: Minimizes environmental impact, potential for deeper resources, may be deployed in most geographies and geologies.
- Cons: Technological challenges, higher costs compared to open-loop systems, may suffer from near-wellbore temperature declines.
- Continental U.S. Fairway Locations: Research and pilot projects in various states, including Nevada and Utah. As with most geothermal technologies, initial targets are high-temperature fairways within the Western US, but with further technological improvements, may be deployable nationwide.

5. Sedimentary Geothermal

Sedimentary geothermal systems involve heat resources hosted in sedimentary rock formations, where heat is generated through rapid burial into high-heat regimes and by radiometric decay. These systems are found in sedimentary basins with elevated temperatures at depth. Sedimentary geothermal play types may include geopressured systems, where elevated temperatures and pressures in sedimentary formations offer strong potential for geothermal energy extraction. Power output per well in these systems may be relatively low given generally lower geothermal gradients (Birdsell et al., 2024).

- Pros: Synergistic use of existing infrastructure, potential for co-production of oil and gas, large, well-studied play fairways.
- Cons: Technical challenges in integrating with existing operations, reservoir compatibility, relatively low heat and resource density.
- Continental U.S. Fairway Locations: Oil fields in California, the Texas Gulf Coast, the Appalachian Basin, and elsewhere.

6. Direct-Use Systems

Direct-use systems utilize geothermal fluids directly for heating purposes, such as space heating, greenhouse operations, and aquaculture. These systems have temperatures less than 100°C, and, because lower geothermal gradients are required, they can be found in myriad geological environments. Single well capacities may be equivalent of up to 2 MW (Moya et al., 2018; Khodayar & Bjornsson, 2024).

- Pros: Lower cost compared to electricity generation, diverse applications, few geographical limitations
- Cons: Limited to areas with suitable heat demand, may require separate distribution systems, small usable radius from resource.
- Continental U.S. Fairway Locations: Technically, geologically and geographically unlimited; typically limited by proximity to facilities and municipalities that may benefit from these systems.

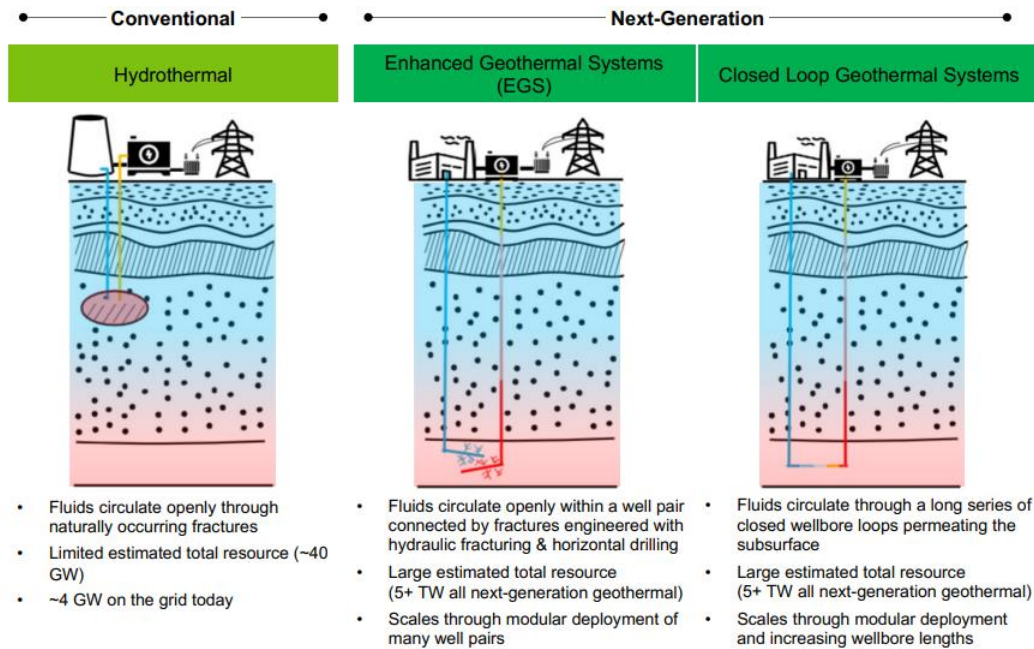


Figure 2-2: Geothermal technology overview across conventional hydrothermal systems (left) and next-generation designs (right). (Source: Blankenship et al., 2024).

2.1.3 Temperature/Depth Ranges

Understanding the relationship between temperature and depth is crucial for assessing geothermal resources and designing geothermal energy systems. This analysis provides an overview of temperature/depth ranges associated with geothermal systems, along with their significance for geothermal exploration and utilization (IPCC, 2011).

1. Shallow Geothermal Resources

Shallow geothermal resources are typically found within the upper few kilometers of the Earth's crust. Temperature/depth ranges for shallow resources vary widely but generally fall within the range of 20 to 200°C at depths of 1 to 3 kilometers. These resources are suitable for direct-use applications such as space heating, aquaculture, greenhouse operations, and hot water supply for industrial processes.

2. Medium-Depth Geothermal Resources

Medium-depth geothermal resources are located at depths of 3 to 5 kilometers below the surface. Temperature ranges for medium-depth resources typically range from 150 to 300°C. These resources may suit direct-use applications or electricity generation using binary cycle power plants.

3. Deep Geothermal Resources

Deep geothermal resources are situated at depths greater than 5 kilometers and often extend into the Earth's mantle. Temperature/depth ranges for deep resources can exceed 300°C, reaching as high as 600°C or more in some cases. Deep resources are primarily used for electricity generation using flash steam or binary cycle power plants.

4. Significance of Temperature/Depth Ranges

Understanding the temperature and depth at which geothermal resources occur provides insights into the suitability and potential of geothermal resources for various applications (Figure 2-3).

Understanding temperature gradients helps in delineating geothermal reservoirs and estimating the energy output of geothermal systems.

Depth considerations are essential for well drilling and reservoir engineering, as deeper resources may require specialized drilling techniques and equipment. Drilling costs increase significantly with depth and can have a significant impact on project economics.

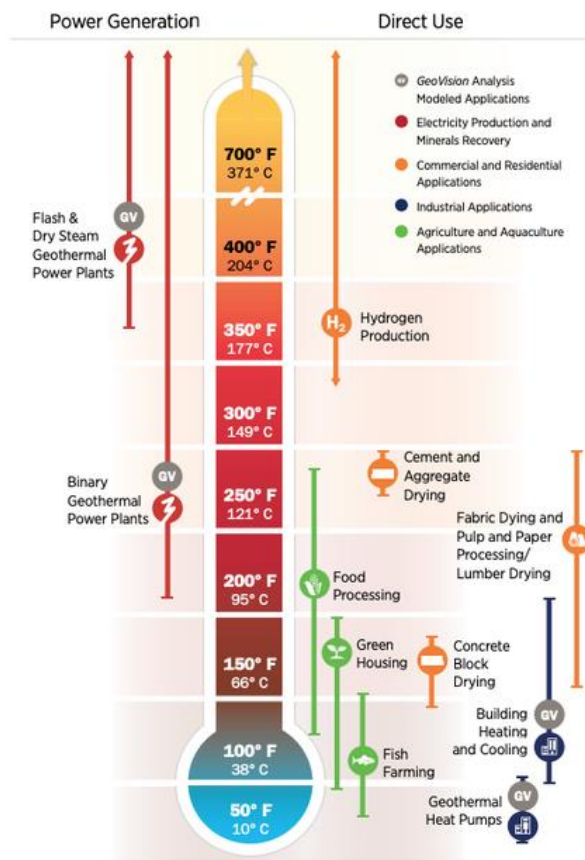


Figure 2-3: Common energy applications based on geothermal temperature ranges (Source: Rizzi, 2023).

2.1.4 Geologic Settings

Understanding the geologic settings conducive to geothermal resource development is essential for successful exploration and utilization.

1. Tectonic Plate Boundaries

Tectonic plate boundaries are the regions of the Earth's crust where tectonic plates interact. Divergent boundaries, characterized by rift zones and mid-ocean ridges, showcase high heat flow and volcanic activity, making them ideal for geothermal exploration (Ingebritsen, 2017). Convergent boundaries, where plates collide, give rise to subduction zones and volcanic arcs, offering geothermal potential in associated metamorphic rocks (Reid, 2013). Transform boundaries, where plates slide past each other, create fault systems that can facilitate fluid circulation and heat transfer, providing additional opportunities for geothermal resource development (Simpson, 1981). Figure 2-4 provides examples of geothermal fields utilizing resources associated with these boundaries.

- Locations in the Continental US:
 - Convergent Boundaries: Found along the west coast of the US, including the Cascadia Subduction Zone and the Aleutian Trench.
 - Transform Boundaries: The San Andreas Fault in California.
- Range of Geothermal Gradients:
 - Convergent Boundaries: Geothermal gradients vary depending on the depth of subduction, faulting, and local presence of magma chambers and other volcanic features.

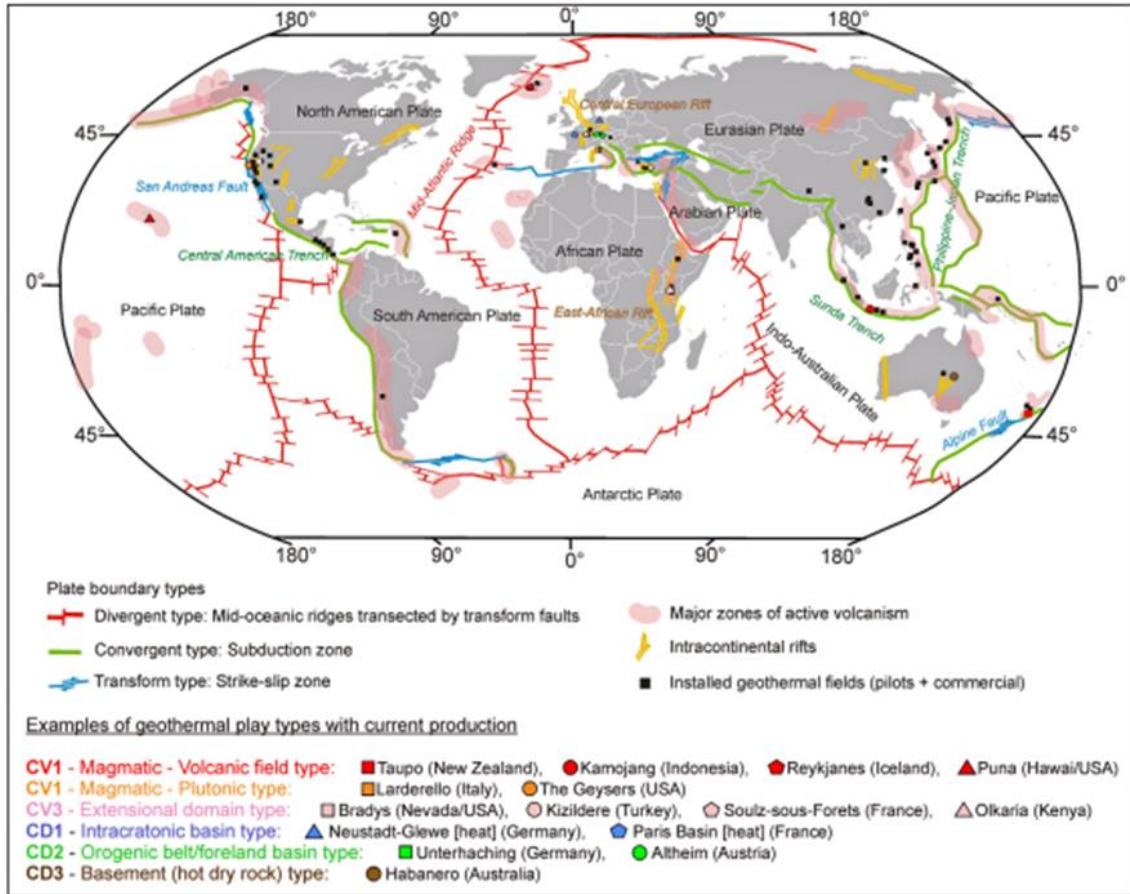


Figure 2-4: Global view of plate tectonic boundary-associated geothermal fields. Note predominance of fields along the west coast of the U.S. (Source: Moeck, 2014).

2. Volcanic Regions

Volcanic regions, including volcanic fields, calderas, and stratovolcanoes, are characterized by high heat flow and magmatic activity. These areas often contain shallow geothermal reservoirs with hot water or steam suitable for power generation.

- Location in the Continental US: Examples include the Yellowstone Caldera in Wyoming, Long Valley Caldera in California, and the Cascades region within California, Oregon, and Washington.
- Range of Geothermal Gradients: Generally high due to the proximity to active magma chambers and volcanic activity (USGS, 2020).

3. Fault Zones

Fault zones are crucial for geothermal exploration in the Great Basin region of the Western US. Faults and Hinz (2015) conducted an inventory of known geothermal systems, revealing that nearly 39% are blind, indicating significant hidden resources. These systems are closely linked to tectonic strain rates, with regions experiencing extensional to transtensional strain hosting most high-temperature activity. The study identifies step-overs in normal fault zones as the most favorable settings, accounting for

approximately 32% of geothermal systems. Understanding these structural settings is essential for identifying and exploring hidden geothermal resources in the region (Faulds & Hinz, 2015).

- Location in the US: Commonly found throughout the country, including the Basin and Range Province in Nevada and the San Andreas Fault in California.
- Range of Geothermal Gradients: Geothermal gradients can vary widely depending on the depth and extent of faulting, with higher gradients typically closer to the surface (Faulds & Hinz, 2015).

4. Sedimentary Basins

The study examines the potential of sedimentary basins for geothermal power generation in the US, an area often overlooked in previous assessments. It highlights the natural porous and permeable characteristics of sedimentary basins, which can host substantial geothermal heat resources.

- Location in the US: Examples include the Williston Basin in North Dakota and Montana and geopressured geothermal systems along the Gulf Coast of Texas and Louisiana (Ogland-Hand, 2024).
- Range of Geothermal Gradients: Geothermal gradients tend to be lower compared to volcanic regions, but can still support geothermal resource development, especially in deeper sedimentary formations (Ogland-Hand, 2024).

2.1.5 Distribution of Geothermal Resources in the US

1. Western United States

States like California, Nevada, Oregon, and Idaho boast significant geothermal resources, as evidenced by the distribution of power plants illustrated in Figure 2-5. The region's geological activity, including tectonic plate boundaries, volcanic terrains, and faults, creates optimal conditions for geothermal energy production (Faulds et al., 2011). This area is marked by geographic features such as geysers, hot springs, and volcanic landscapes. These states accommodate numerous geothermal power plants and harbor some of the nation's largest geothermal fields.

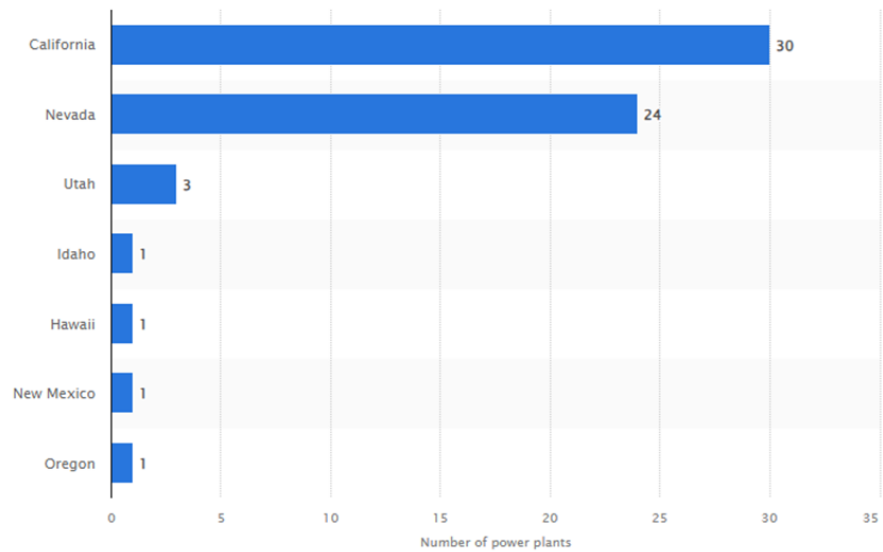


Figure 2-5: Number of geothermal power plants in the United States as of 2021, by state (Fernández, 2024).

2. Great Basin Region

The Great Basin region, encompassing parts of Nevada, Utah, and eastern California, is known for its extensive geothermal resources, with existing geothermal power plants and capacity exceeding 600 MW. Since many geothermal resources in the region are blind (lacking surface indicators like hot springs), the region is thought to have significant further resource potential (Faulds et al., 2016).

3. Rocky Mountains

The Rocky Mountain region, spanning western states including New Mexico, Colorado, Wyoming, and Montana, also hosts geothermal resources. While not as prolific as the western US, the region has favorable geological characteristics, including Neogene volcanism, Quaternary faulting, and high heat flow. The presence of mafic and silicic magmas, along with Quaternary faulting and regional high heat flow, further enhance the area's suitability for geothermal resources (Morgan, 2011).

2.1.6 Factors Influencing Cost of Geothermal Power

1. Resource Characteristics

The temperature, depth, permeability, rock mechanics and connectivity of geothermal reservoirs influence the cost of geothermal power generation. High-temperature reservoirs with shallow depths and good permeability are generally associated with lower development and operational costs than the deeper, lower temperature plays (Tester, 2006).

2. Exploration and Drilling

The cost of exploration activities, including geological and geophysical surveys and exploratory drilling, can significantly impact the overall cost of geothermal projects. Deep drilling in search of suitable reservoirs may incur high upfront costs (Tester, 2006).

3. Reservoir Engineering and Well Stimulation

Enhanced geothermal systems (EGS) and other reservoir engineering techniques aimed at improving heat extraction efficiency may involve additional costs for well stimulation, hydraulic fracturing, and reservoir management (Blankenship et al., 2024).

4. Power Plant Construction and Operation

The construction and operation of geothermal power plants, including steam turbines, generators, and associated infrastructure, contribute to the overall cost per MW of geothermal power generation.

5. Estimated Cost per MW for Geothermal Power in the US

The cost of geothermal energy in the US varies depending on factors such as resource quality, location, technology employed, and project scale. Generally, geothermal energy is considered competitive with other renewable energy sources, with costs between \$61 and \$102 per megawatt-hour (MWh) (Lazard, 2023; Figure 2-6).

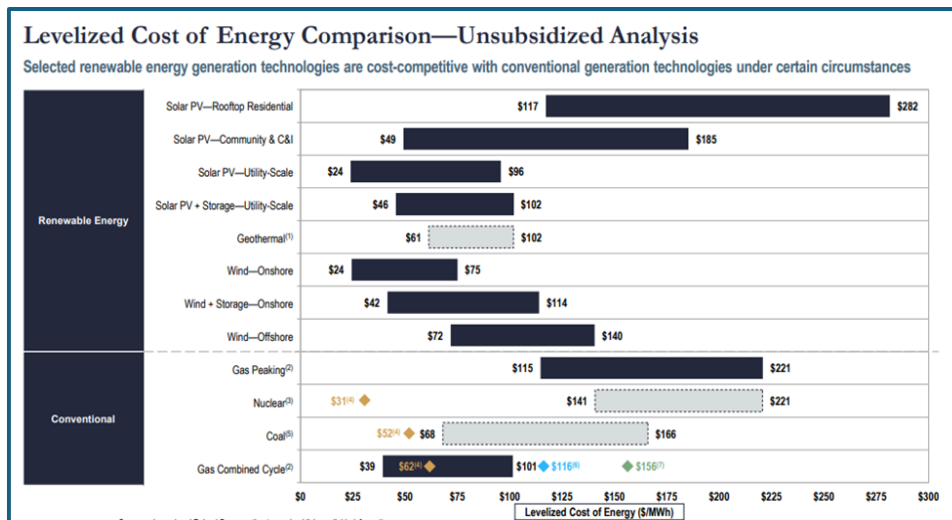


Figure 2-6: Levelized cost of energy comparison—unsubsidized analysis (Source: Lazard, 2023).

Future cost reductions in next-generation geothermal are driven by iterative operational improvements and new technical advancements (Figures 2-7 and 2-8). These advancements aim to make enhanced geothermal systems cost competitive with other clean firm sources. In 2021, the U.S. Department of Energy (DOE) launched the Enhanced Geothermal Shot™ as part of the Energy Earthshots Initiative™, aiming to reduce the cost of geothermal power to \$45/MWh by 2035 (Blankenship, 2024).

The Enhanced Geothermal Shot targets a 90 percent reduction in the cost of Enhanced Geothermal Systems (EGS) by 2035, aiming for an effective Levelized Cost of Electricity (LCOE) of \$45/MWh.

Current cost reductions exceed expectations, with the Overnight Capital Cost (OCC) estimate dropping from \$27,800 per kW in 2021 to approximately \$14,700 per kW in 2023.

Field evidence suggests that improvements in geothermal drilling, well field stimulation, and economies of scale from potential plant size enhancements have been major drivers of cost reduction.

These technology improvements not only benefit EGS but also contribute to cost reductions in exploration drilling and well drilling across EGS and closed-loop geothermal systems.

Figure 2-7: Future cost reduction, modified from Blankenship (2024).

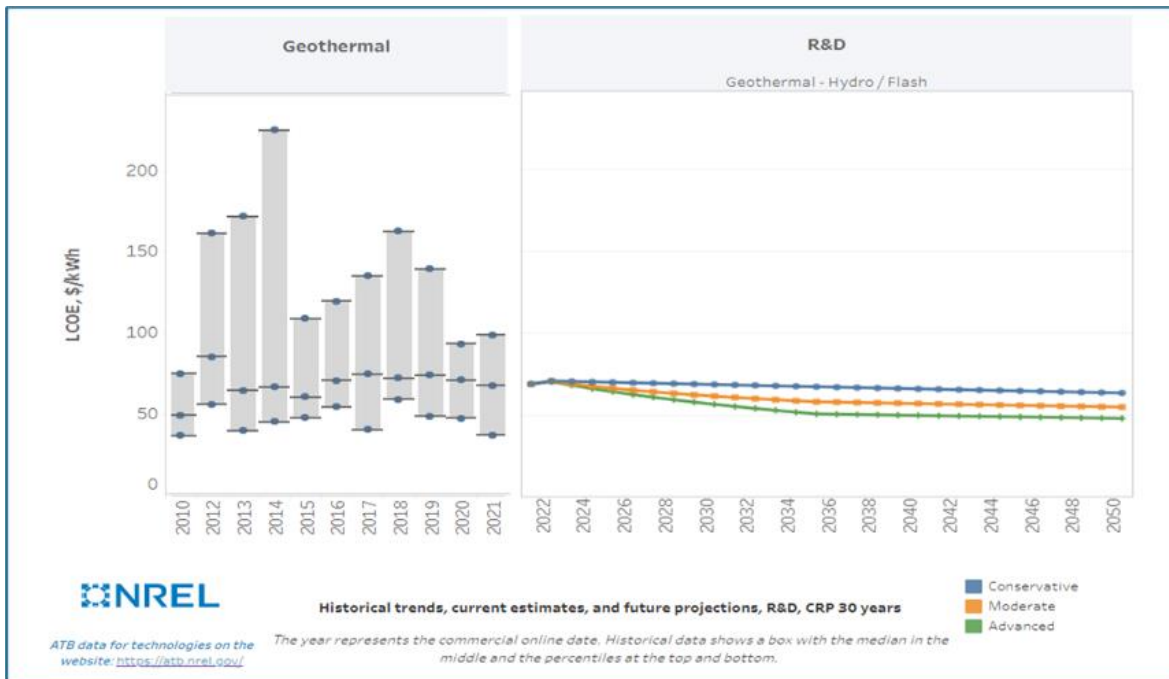


Figure 2-8: 2023 Historical LCOE by NREL annual technology baseline.

2.1.7 Geothermal Power Plants

There are two main methods to convert geothermal heat to electricity: flash plants and binary-cycle plants. Flash plants produce steam directly from geothermal fluids, using the steam to drive turbines and generate electricity. They are ideal for higher-temperature systems and are cost-effective because they require few wells and are simple in design (NREL, 2023; Table 2-1). Binary cycle plants generate electricity by utilizing a secondary fluid with a lower boiling point than water, heated by geothermal energy to generate power through an organic Rankine cycle. They are suitable for lower-temperature systems but are costlier due to their complexity and the need for more wells.

Table 2-1: Geothermal Resource and Cost Characteristics (Source: National Renewable Energy Laboratory, 2023).

Technology	Temperature (°C)	>=200°	150–200°	135–150°	<135°
Hydrothermal	Number of <i>identified</i> sites	20	21	17	57
	Total <i>identified</i> capacity (MW)	3,824	783	378	581
	Average overnight capital cost, or OCC (\$/kW)	4,127	9,084	9,672	17,921
	Min OCC (\$/kW)	2,893	4,598	7,702	12,043
	Max OCC (\$/kW)	5,922	37,143	11,932	25,364
	Example of plant OCC (\$/kW) *	4,547	6,043	N/A	
	Number of <i>undiscovered</i> sites	7	8	2	17
	Total <i>undiscovered</i> capacity (MW)	14,909	4,340	339	6,223

Table 2-1 (continued): Geothermal Resource and Cost Characteristics (Source: National Renewable Energy Laboratory, 2023).

Technology	Temperature (°C)	>=200°	150–200°	135–150°	<135°
		Average OCC (\$/kW)	3,446	7,031	9,746
	Min OCC (\$/kW)	3,133	6,398	9,746	14,325
	Max OCC (\$/kW)	4,276	7,877	9,746	22,452
Shallow EGS	Number of sites	12	20	N/A	
	Total capacity (MW)	787	707		
	Average OCC (\$/kW)	7,770	22,501		
	Min OCC (\$/kW)	6,139	16,329		
	Max OCC (\$/kW)	11,975	33,431		
	Example of plant OCC (\$/kW)	9,650	19,449		
Deep EGS (3–7 km)	Number of sites	N/A	N/A	N/A	
	Total capacity (MW)	100,000+			
	Average OCC (\$/kW)	20,848	49,155		
	Min OCC (\$/kW)	14,562	25,197		
	Max OCC (\$/kW)	33,687	88,318		
	Example of plant OCC (\$/kW)	11,748	27,822		

2.2 Fundamentals of CO₂ Geologic Storage

2.2.1 Geologic Settings

The selection of appropriate geological settings is crucial for the success and safety of carbon capture and storage (CCS) projects. Key considerations include porosity, thickness, permeability, and continuity of storage formations, and caprock layer integrity to prevent CO₂ leakage. Protecting other minerals, energy, and groundwater resources from contamination by CO₂ is essential by ensuring the CO₂ is retained in the reservoir (Bachu, 2008). Static Earth Modeling (Figure 2-9) using subsurface data and cutting-edge technologies reduces several risks and improves the performance of the storage operations.

The three major types of rock—igneous, metamorphic, and sedimentary—are targeted for storage formations in CCS projects. Each type varies in its capacity, injectivity, geochemistry, and integrity, with porosity and permeability being critical factors. Integrity is paramount for confining fluids or gases within a geologic unit to prevent migration to lower-pressure areas such as underground sources of drinking water (USDWs), petroleum reservoirs, or the surface. Proper evaluation of these criteria is essential for identifying suitable storage formations and avoiding potential leaks (IPCC, 2005).

Depleted oil and gas fields can also be suitable for CCS since they have proven trapping mechanisms and may have existing infrastructure. However, storage capacity may be limited by pressure constraints, especially in depleted reservoirs, where the integrity of existing wellbores may cause heightened leakage risk. Enhanced oil recovery (EOR) operations offer economic benefits and may offset storage costs.

Table 2-1 (continued): Geothermal Resource and Cost Characteristics (Source: National Renewable Energy Laboratory, 2023).

The CO₂ storage target favored by many project developers is deep saline aquifers. These aquifers provide large storage capacities, generally have few existing wellbore penetrations, and exist in most sedimentary basins, making them far more widespread than depleted petroleum reservoirs.

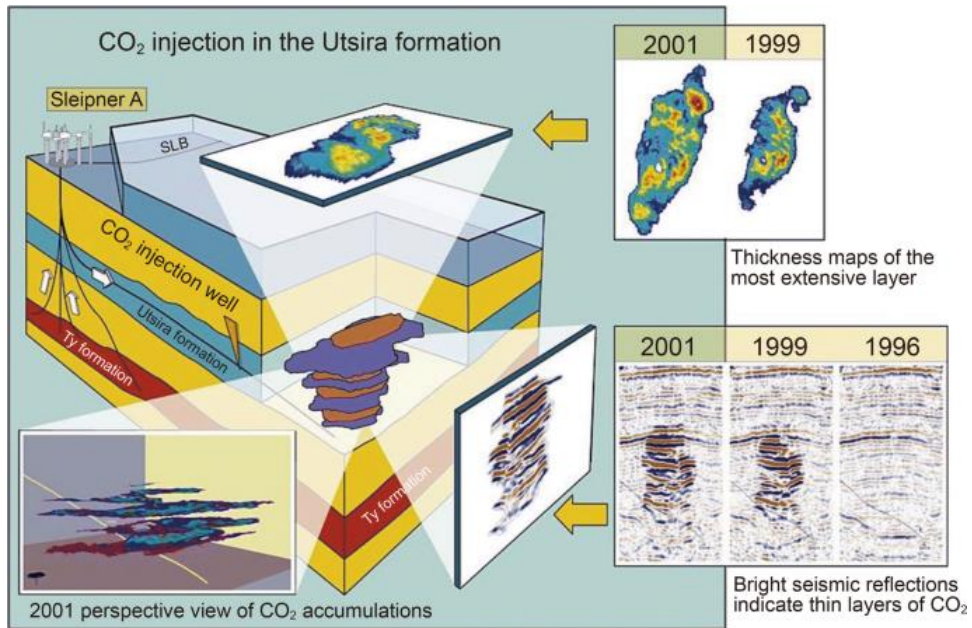


Figure 2-9: Example of Static Earth Modeling using subsurface data (Source: Ajayi, 2019).

2.2.2 Temperature and Depth Ranges for Geological Carbon Storage

Temperature and depth are crucial considerations in CCS projects, as these parameters impact the stability of the reservoir system and the behavior of the stored CO₂.

Geologic Stability: Understanding temperature and depth ranges helps assess the stability of reservoir and caprock formations. Typically, deeper formations experience higher temperatures, which can influence rock properties such as porosity, permeability, formation mineralogy, and the presence and behavior of structural features such as faults and fractures. Assessing these properties within both the target reservoir and overlying caprock ensures the long-term containment of injected CO₂ (IEA, 2009).

CO₂ Density: Temperature and depth influence the behavior of CO₂ within storage formations. In deeper, higher-temperature formations, CO₂ may exist in a supercritical state, where it exhibits both gas and liquid properties (Figure 2-10). This density increase in deeper depths allows for greater volumes of CO₂ to be stored within the same geological volume, optimizing storage efficiency.

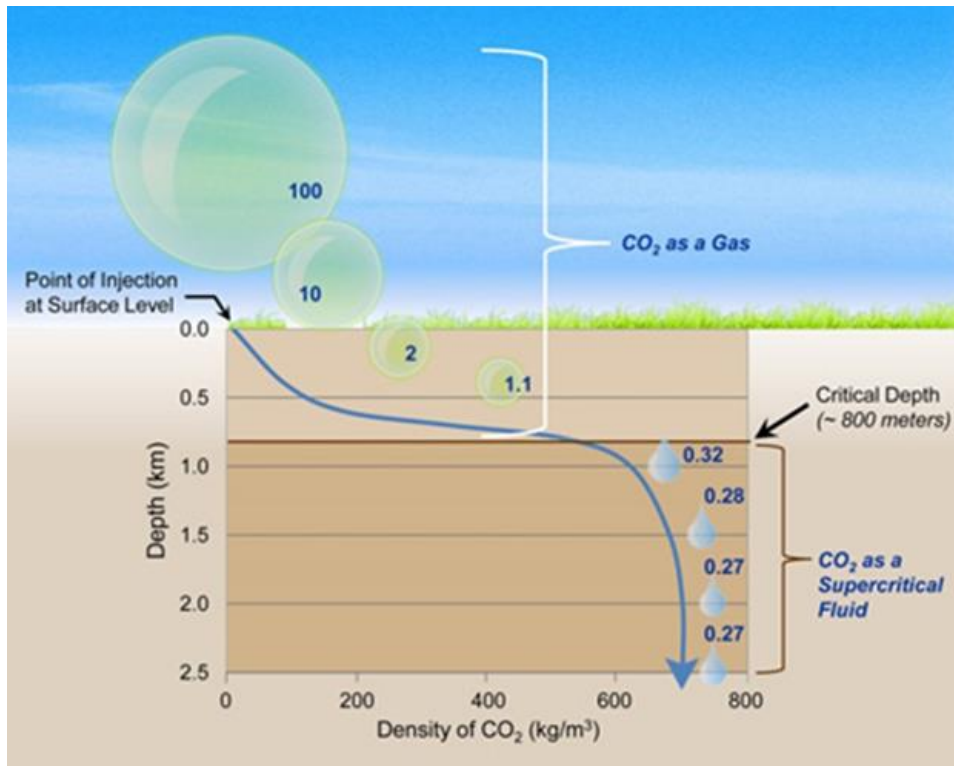


Figure 2-10: Graph showing relationship between CO₂ density and subsurface depth. As depth increases, so does density, making deeper storage reservoirs generally preferable to shallow reservoirs. (Source: National Energy Technology Laboratory, 2024).

For CCS projects, depth ranges can vary depending on the geological formations targeted for storage. Minimum depth ranges for CCS are typically constrained by a supercritical depth threshold (if supercritical conditionals are desired) and/or the base of USDWs. USDWs are defined as any water source containing total dissolved solids of less than 10,000 mg/L (U.S. EPA, 2018). Below are the typical depth ranges.

Shallow Depth Ranges (0-500 meters / 0-1640 ft): CCS projects at shallow depths are typically associated with coal bed methane reservoirs and depleted oil and gas fields, although studies are ongoing to understand potential for shallow storage within basalt formations. The temperature ranges at these depths are relatively low, typically within the range of 20°C to 80°C, and CO₂ storage occurs in the gas phase or via mineralization in basalts.

Intermediate Depth Ranges (500-1500 meters / 1640- 4921 ft): CCS projects at intermediate depths involve saline aquifers and deep sedimentary formations. Temperatures at these depths range from approximately 50°C to 100°C, depending on the geothermal gradient and local geology.

Deep Depth Ranges (>1500 meters / 4921 ft): CCS projects at deep depths are associated with deep saline aquifers, basalt formations, and depleted petroleum reservoirs. Temperatures in these formations can exceed 100°C and may reach up to 200°C or higher.

Extreme Depth Ranges (>3000 meters / 9842 ft): In some cases, CCS projects may target ultra-deep geological formations, such as deep ocean sediments or subduction zones. Temperatures at these extreme depths can exceed 200°C.

2.2.3 Play Types

Figure 2-11 shows an example of the various play types, which include depleted oil and gas reservoirs, deep saline aquifers, unmineable coal seams, basalt formations, and shale formations (IPCC, 2005).

Depleted Oil and Gas Reservoirs: Utilizing depleted oil and gas reservoirs for CCS involves injecting CO_2 into formations that previously contained hydrocarbons. These reservoirs offer suitable porosity, permeability, and retention for CO_2 storage.

Deep Saline Aquifers: Saline aquifers located deep underground represent vast storage potential for CO_2 . These formations typically exhibit high porosity and low permeability, making them suitable for long-term CO_2 storage (Holloway, 2010).

Unmineable Coal Seams: Unmineable coal seams can provide CO_2 storage. CO_2 can be injected into the seams, displacing methane and adsorbing onto coal surfaces, thus providing a mechanism for long-term storage (Bachu, 2003).

Deep Basalt Formations: Basalt formations offer unique advantages for CO_2 storage due to their reactive properties. CO_2 can react with minerals in basalt, forming stable carbonate minerals and providing long-term storage potential (Goldberg, 2008). Many types of enhanced mineralization require additional research (DOE FECM, 2022; Sandalow et al., 2021).

Organic-rich Shales: Preliminary laboratory testing indicates that the organics in shales have an affinity for CO_2 , allowing for CO_2 absorption and adsorption into microporous shales (Kang et al., 2011). Significant laboratory and field testing is needed to confirm the storage capabilities of shale resources.

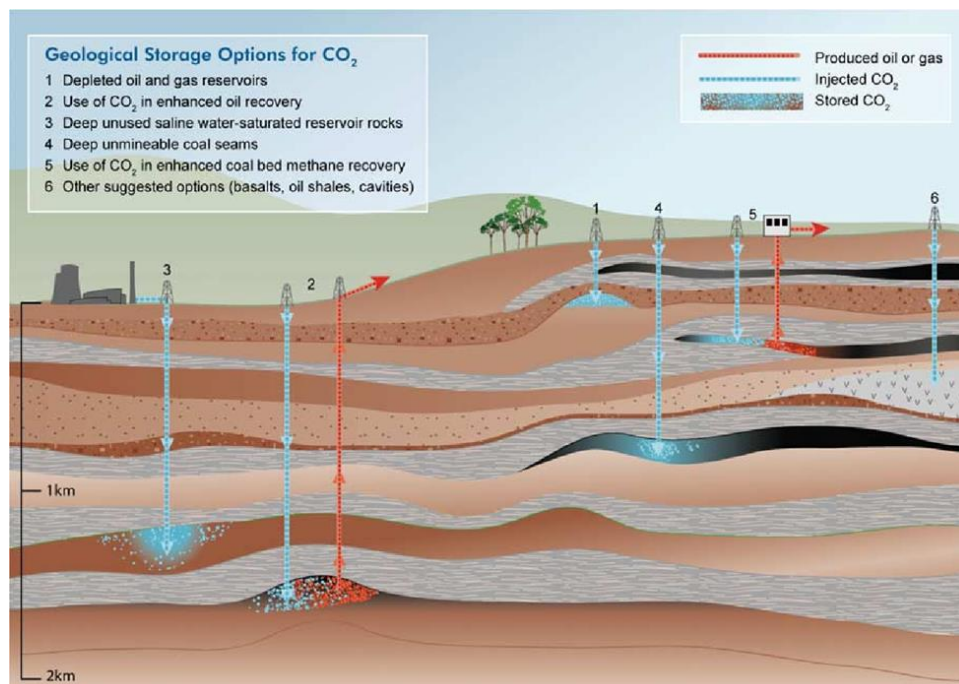


Figure 2-11: Options for geological storage of CO_2 (Benson, 2016).

2.2.4 Geographic Locations of Carbon Storage Fairways

The US offers diverse geographic locations suitable for CCS projects, encompassing various geological formations and regions with different characteristics. The National Energy Technology Laboratory's Carbon Storage Atlas highlights assessed and non-assessed areas of basalt formations, shales, unmineable coals, and depleted reservoirs (NETL, 2016). Resource estimates for these reservoirs were compiled by the Regional Carbon Storage Partnerships (NETL, 2015, Figure 2-12). Regional Initiatives also have additional up-to-date carbon storage resource estimates. Below are some of the notable carbon storage fairway regions, although potential for carbon storage development continues to be evaluated.

Gulf Coast Region: Known for its extensive oil and gas infrastructure, the Gulf Coast region offers both depleted oil and gas fields suitable for CCS and a number of saline aquifers with significant storage potential (Alonzo et al., 2022; McPherson et al., 2005). Significant existing infrastructure such as fields and pipelines, as well as a workforce that is familiar with drilling and subsurface operations make this region optimal for carbon storage.

Midwest Region: The Midwest region, including states such as Ohio, Michigan, and Pennsylvania, features deep saline aquifers suitable for large-scale CO₂ storage. These formations offer ample capacity for sequestering CO₂ captured from industrial sources in the region (Bauer, 2012). There is also potential for enhanced coalbed methane recovery (Rose, 2010).

Southeast Region: Sites in this region include deep saline formations and depleted petroleum reservoirs. There is also potential for enhanced coalbed methane recovery (Rose, 2010).

Southwest Region: States throughout the southwest have both deep saline aquifers and depleted oil and gas reservoirs that are suitable for CCS projects. The region's vast open spaces and extensive existing oil and gas infrastructure facilitate CCS implementation (USGS, 2013).

West Coast Region: This region features deep saline formations suitable for CO₂ storage and may have some potential in depleted petroleum reservoirs. Additionally, the region's volcanic formations offer potential for basalt mineralization (Goldberg, 2018).



Figure 2-12: US Regional Carbon Sequestration Partnership areas (NETL, 2015).

2.2.5 Range of Geological Carbon Storage Potentials

The storage potential of basins targeted for CCS varies widely depending on available geological formations, tectonics and other regional characteristics. Assessing the range of storage potential per square mile provides valuable insights into the capacity of different areas to sequester CO₂ effectively. State surveys and Regional Carbon Sequestration Projects have determined high-level storage resource estimates. The USGS (2013) compiled some of this data to output ranges in carbon storage resource estimates (Figure 2-13). Each basin has a minimum storage estimate of 100 megatonnes (Mt) to as much as 1,000 gigatonnes (Gt).

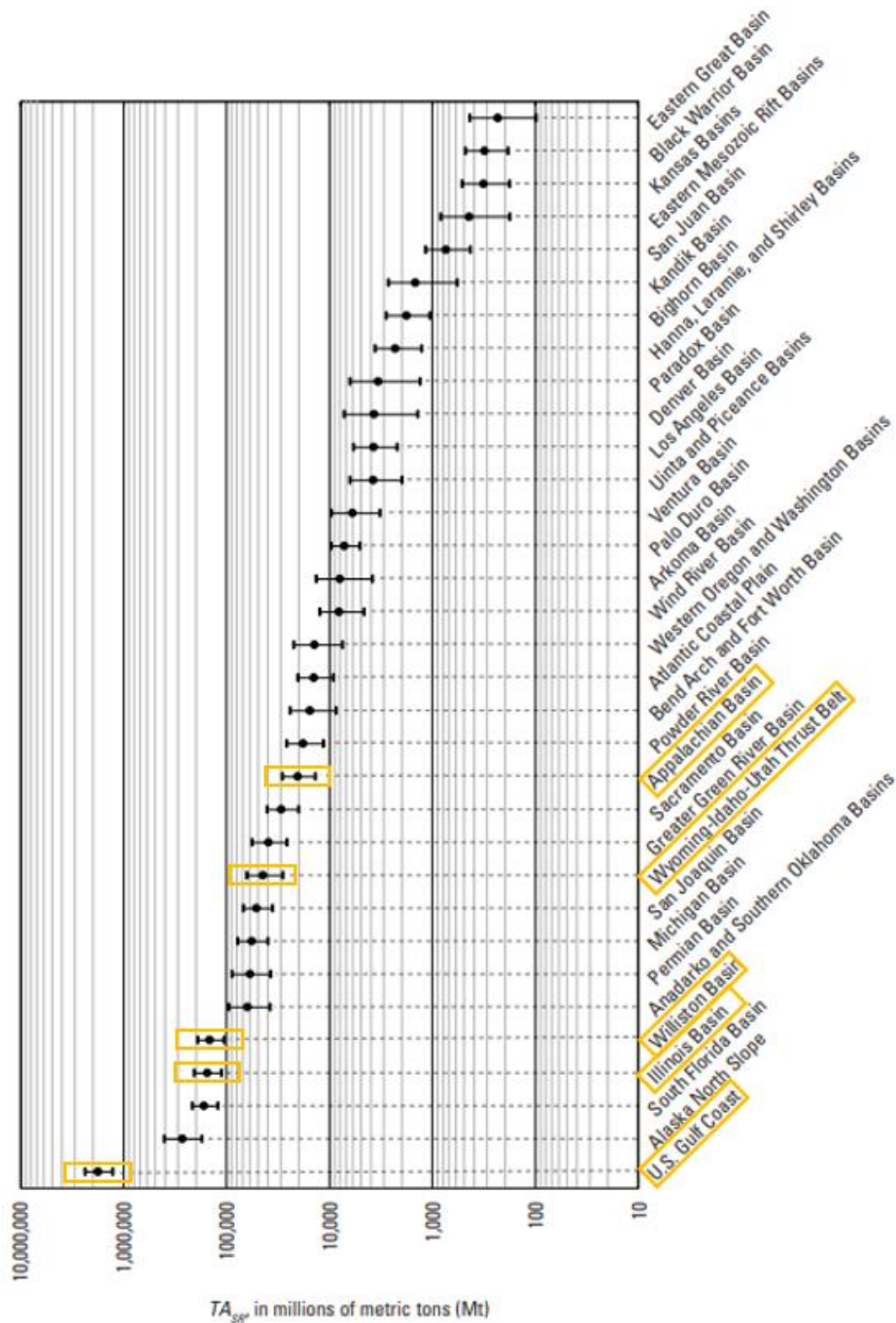


Figure 2-13: P5-P95 estimates of carbon storage potential for key basins within the United States. Basins at the top of the graph have relatively low storage capacities, while basins at the bottom of the graph have large capacities. Basins of note include the U.S. Gulf Coast Basin with over 1,000 billion metric tons of accessible storage, the Illinois and Michigan basins in the Midwest, the Williston and Thrust Belt basins in the Rockies regions, and the Appalachian Basin in the eastern U.S. (modified from USGS, 2013).

2.2.6 Estimated Cost per Tonne of Stored CO₂

The estimated cost per tonne of stored CO₂ in CCS projects varies depending on factors such as storage type, depth of injection, distance to transportation infrastructure, and local regulatory conditions. Generally, the cost includes expenses related to capture, transportation, injection, monitoring, and verification of CO₂ storage (IEA CCS Roadmap, 2020).

Capture Costs: These costs include capturing CO₂ from point sources such as power plants or nonpoint sources such as DAC facilities. Estimates for capture costs range from \$20 to \$100 per tonne (Figure 2-14; Congressional Budget Office, 2023).

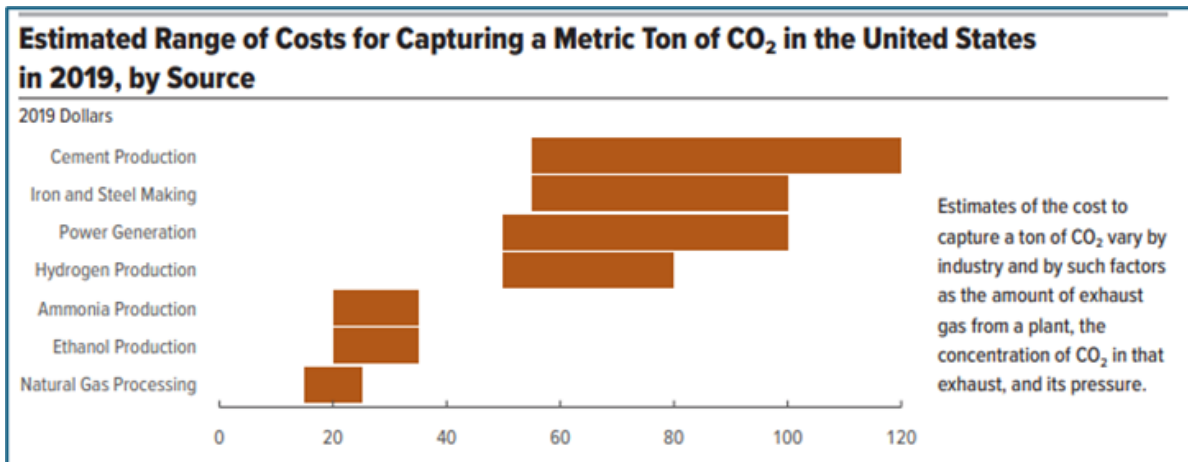


Figure 2-14: Estimated range of CO₂ capture costs (Data source: Congressional Budget Office, 2023).

Transportation Costs: After capture, CO₂ is transported to storage sites via pipelines or other means such as trucking, rail, or shipping. Transportation costs vary depending on transportation type, distance to storage sites, topography, and the availability of existing infrastructure. Estimated transportation costs range from \$5 to \$20 per tonne (IEA, 2020).

In CCS projects, pipeline transportation costs vary based on factors such as volume, pipeline specifications, labor, and lifespan. Location and geography also impact costs significantly. Typically, transport expenses make up a small portion, usually less than one-quarter, of total CCS project costs. Figure 2-15 shows a range of relative CO₂ pipeline transport costs.

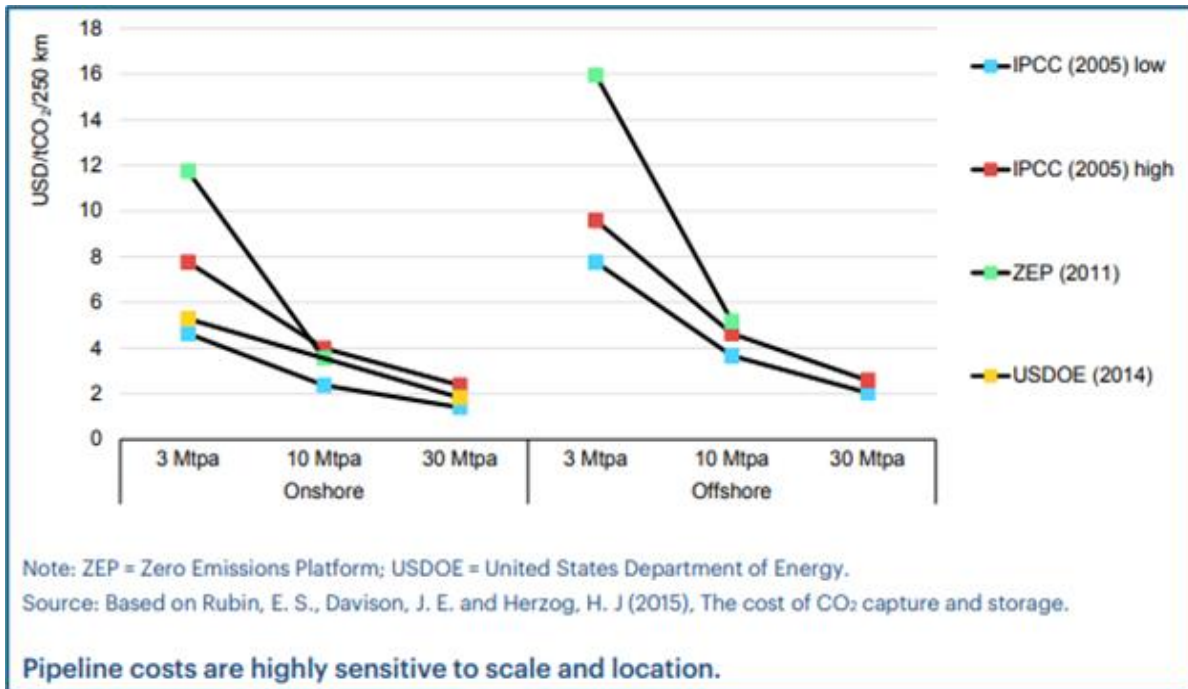


Figure 2-15: Indicative unit CO₂ pipeline transport costs (IEA, 2020).

Injection Costs: Once transported, CO₂ must be injected into underground storage reservoirs. Injection costs include expenses related to drilling wells, reservoir characterization, and injection operations. Costs range from \$5 to \$30 per tonne of CO₂ injected, depending on reservoir depth and geologic conditions (Global CCS Institute, 2021).

Monitoring and Verification Costs: Continuous monitoring and verification are essential to ensure the integrity of CO₂ storage sites and compliance with regulatory requirements. Monitoring costs can vary widely but may range from \$1 to \$10 per tonne of CO₂ stored annually (Global CCS Institute, 2021).

Site-Specific Costs: Additional site-specific factors, such as site characterization, permitting, and regulatory compliance, can significantly impact overall project costs. These costs are highly variable and depend on local geological, environmental, and regulatory conditions.

2.3 Fundamentals of DAC systems

2.3.1 Range of DAC Technologies

Two technological approaches are currently being used to capture CO₂ from the atmosphere: liquid and solid DAC. Figures 2-16 and 2-17 provide examples of two common liquid DAC (L-DAC) systems, while Figure 2-18 shows a typical solid DAC (S-DAC) process.

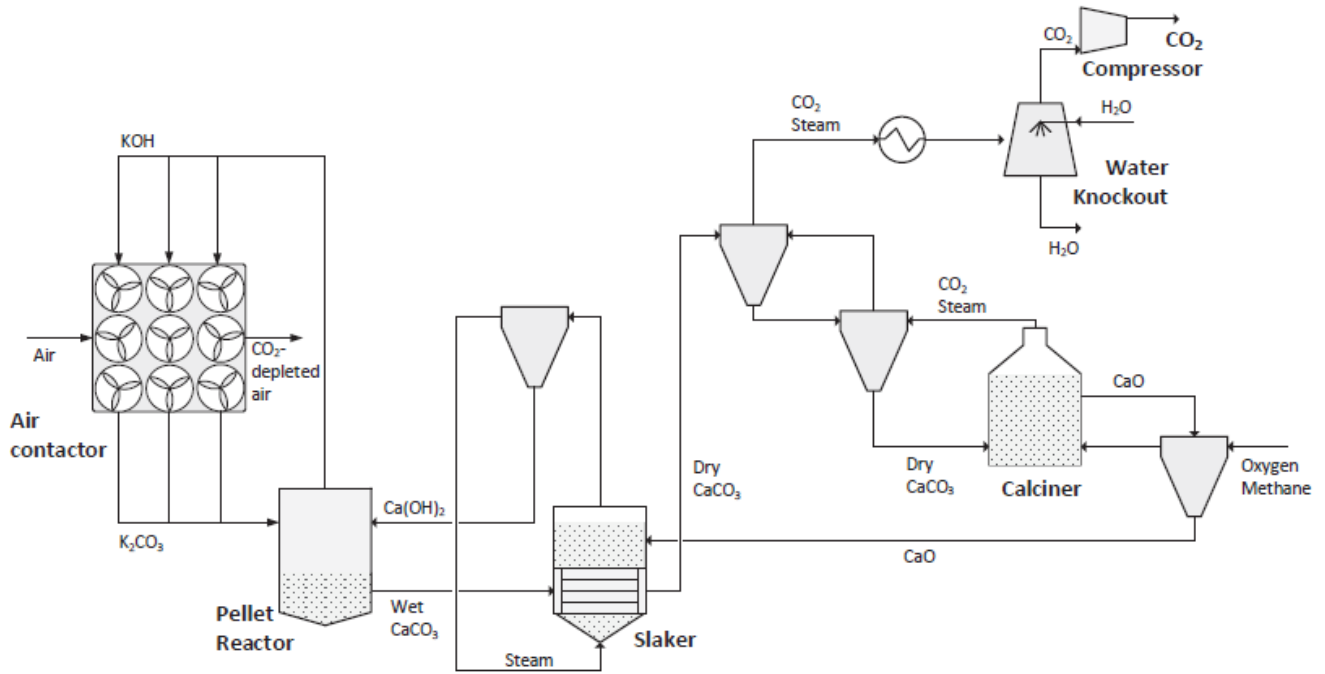


Figure 2-16: Typical alkali-scrubbing liquid DAC process (Sabatino et al., 2021).

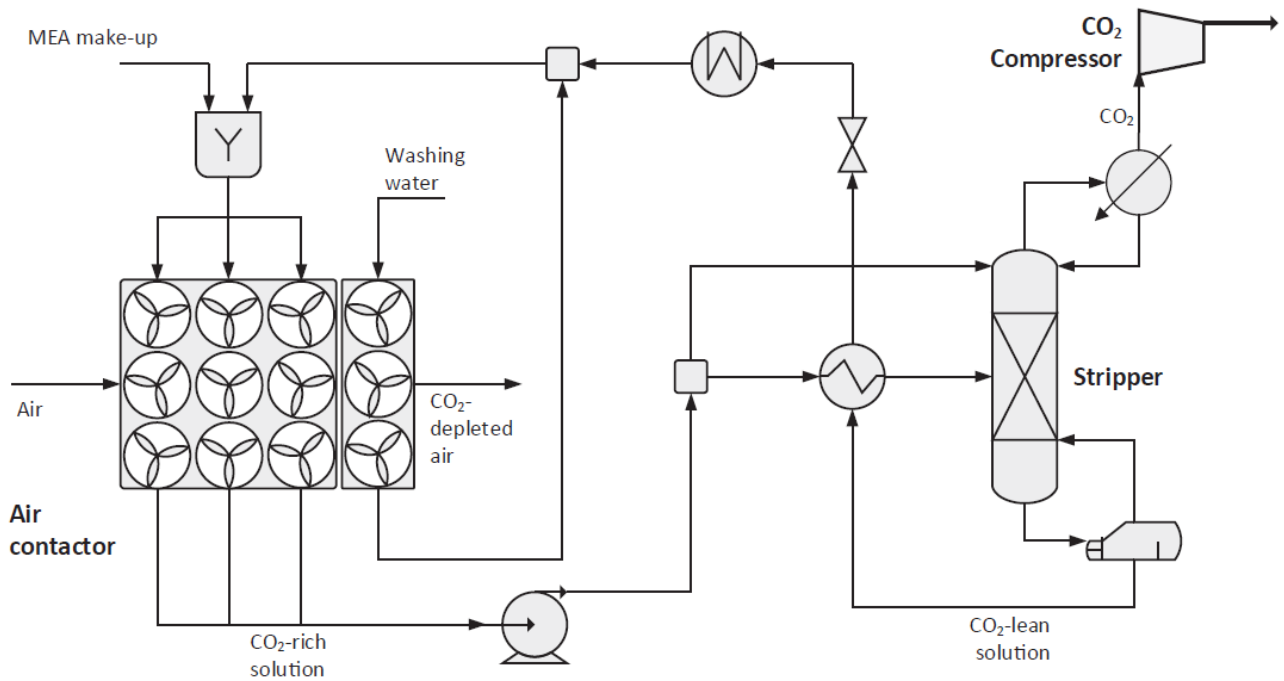


Figure 2-17: Typical amine-scrubbing liquid DAC process (Sabatino et al., 2021).

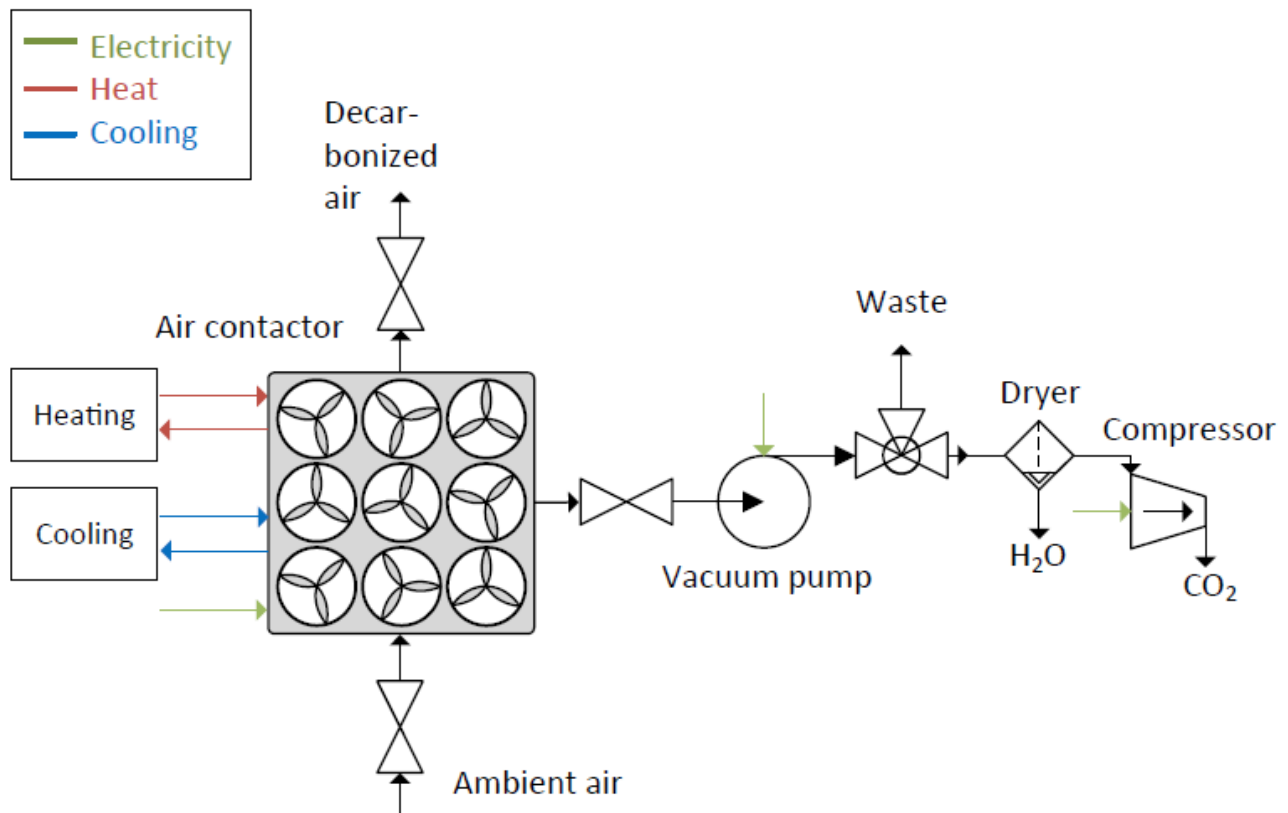


Figure 2-18: Example of a solid sorbent DAC system (Sabatino et al., 2021).

Liquid DAC (L-DAC): L-DAC uses an aqueous basic solution (typically either amine or alkali based), releasing absorbed CO₂ through a series of high temperature units operating between 300 and 900°C. The steps of a general alkali-based L-DAC process are provided: CO₂ is reacted with the basic solution to form a carbonate. The carbonate is then precipitated (e.g., calcium carbonate) in a causticizer while the solvent is regenerated for reuse. The precipitate next is heated (about 900°C) to release CO₂ (Bertoni et al., 2024). Additional processing steps may be needed depending on CO₂ output requirements (e.g., purity, transportation, and storage). An amine-based L-DAC system is simpler than the alkali system; an amine solvent contacts with air to adsorb the CO₂ which is then sent to a stripping unit to separate the CO₂ and regenerate the solvent (Sabatino et al., 2021; Mostafa, et al., 2022).

Solid DAC (S-DAC): S-DAC utilizes solid adsorbents operating at ambient to low pressure (0.2-1.4 bar) and medium temperature (80-130°C) (Fasihi et al., 2019; Sabatino et al., 2021). These S-DAC systems work by contacting as much of the ambient air as possible with the solid sorbent (typically amine based) to adsorb CO₂ from the air. Once the solid sorbent has reached capacity, the sorbent unit undergoes a temperature increase and pressure decrease to remove the CO₂ from the sorbent and sends the CO₂ for further processing. The remaining sorbent can then be reused once in ambient conditions to again capture CO₂ from the air (Figure 2-19). The temperature and pressure change of the sorbent unit is often called a vacuum-pressure temperature swing adsorption (VTSA) cycle (Sabatino et al., 2021). This is one of the most popular S-DAC methods but there are others such as the use of a moisture swing adsorption (MSA), which uses water content to remove CO₂ from the sorbent instead of temperature and pressure (Fasihi et al., 2019).

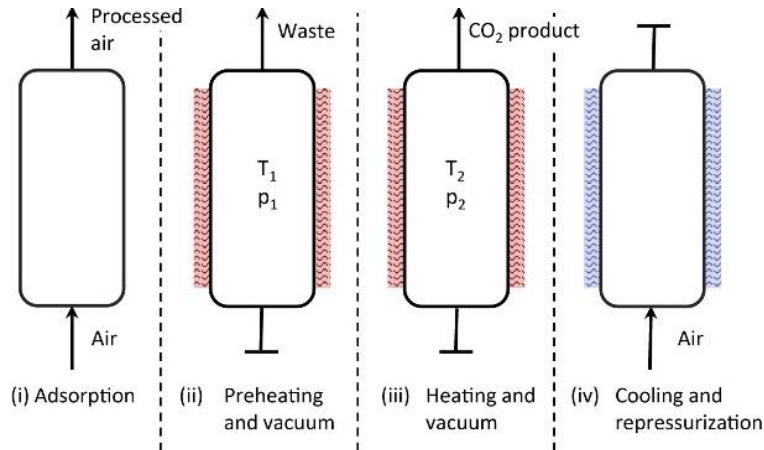


Figure 2-19: VTSA cycle schematic shown as four steps to capture CO₂ from ambient air and regenerate the sorbent (Sabatino et al., 2021).

The S-DAC systems have lower heat capacities but higher energy requirements and are relatively newer compared to the L-DAC systems. Further research is also needed to ensure sorbent stability over time (Sabatino et al., 2021).

2.3.2 Range of DAC Operating Temperatures

Most DAC processes capture CO₂ at ambient temperatures, yet the release of CO₂ from the adsorbent material or resulting units can be highly temperature and process dependent. Solid sorbent systems require lower heat than their liquid counterparts to release CO₂, operating at temperatures between 70 and 150°C. The liquid-based systems require much higher heat operating between 300 and 900°C (Sabatino et al., 2021; Kuru et al., 2023; U.S. DOE, 2023; Fasihi et al., 2019). Figure 2-20 shows some current DAC companies, their DAC technology employed, and corresponding temperatures required to regenerate the captured CO₂ (Fasihi et al., 2019).

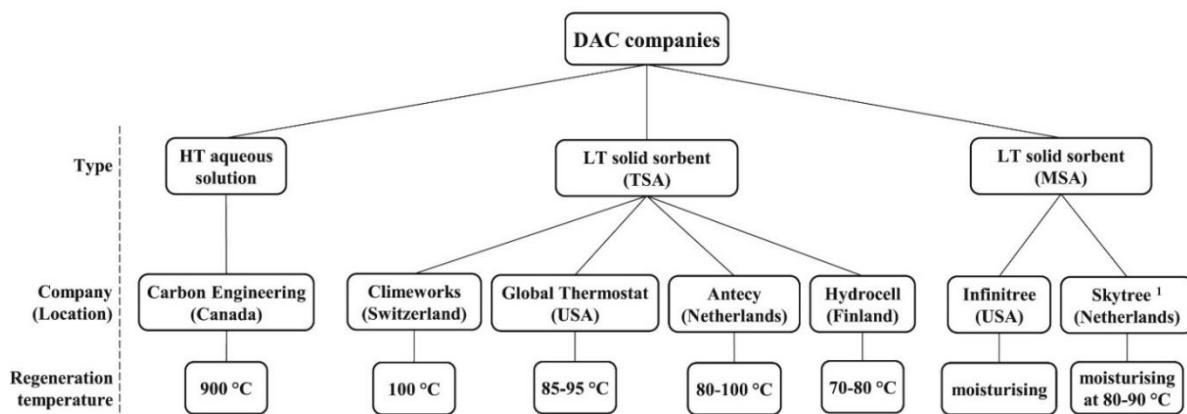


Figure 2-20: DAC technology, ranked as high temperature (HT) or low temperature (LT), used by companies and their CO₂ regeneration temperatures (Sabatino et al., 2021).

2.3.3 Impact of Local Climate on DAC Operations

The local climate, specifically the temperature and humidity, at a DAC facility also impacts operations. Facilities operating in climates at higher temperatures may see a lowered heating demand. However, raised temperatures result in decreased CO₂ adsorption to the sorbent and may require additional cooling costs (U.S. DOE, 2023; Fasihi et al., 2019).

Humidity can affect the S-DAC system positively or negatively. In dry climates, S-DAC systems can reuse their produced water (process by-product). However, in humid climates the facilities need to account for excess produced water (Kuru et al., 2023). Additionally, there is an uptake in CO₂ adsorption at high humidities due to the dilution of CO₂ by the water content. The additional water content in the air decreases the partial pressure of CO₂ which allows for more adsorption. Also, some S-DAC sorbents are less likely to be degraded by O₂ at higher humidities (Kuru et al., 2023; Wurzbacher et al., 2016).

2.3.4 Energy Consumption Range

For DAC facilities the energy requirements depend largely on the type of DAC system. Typically, S-DAC systems are more energy intensive than L-DAC systems operating at 7.2 to 9.5 gigajoules per tonne of CO₂ (GJ/tCO₂) and 5.5 to 8.8 GJ/tCO₂, respectively (Kuru et al., 2023). For both DAC types, much of this energy requirement is due to heating the units (about 5.3 GJ/tCO₂ for L-DAC and 7.2 GJ/tCO₂ for S-DAC) which can be seen in Figure 2-21 (IEA, 2023). Other energy is required for processes such as fluid pumps, fans to process high volumes of air, and CO₂ compression.

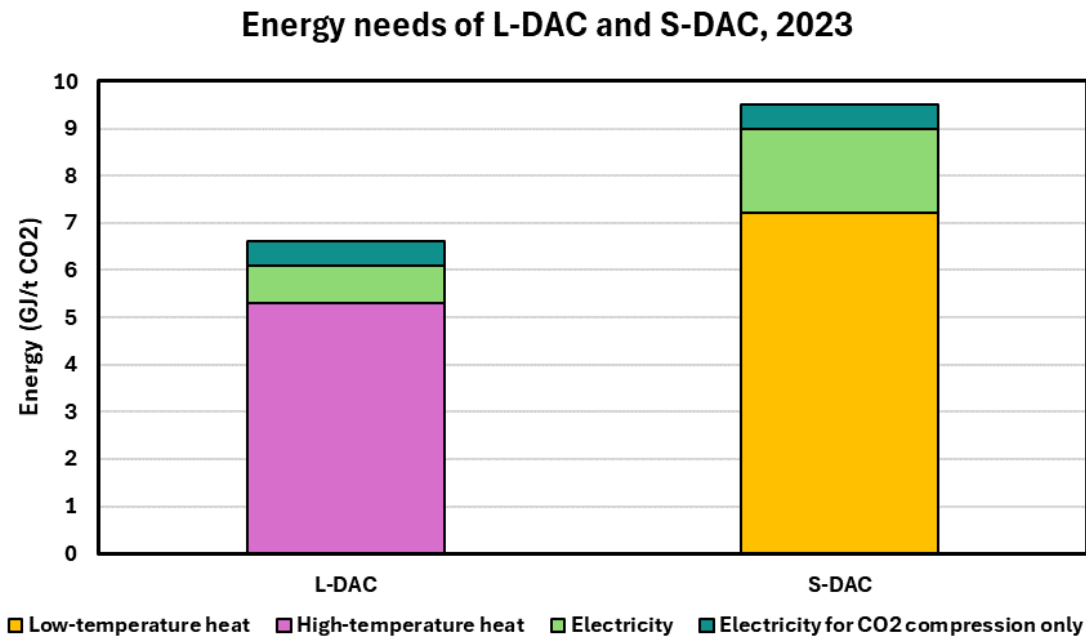


Figure 2-21: Energy requirement per ton CO₂ captured (IEA, 2023).

2.3.5 Estimated Cost per Tonne for DAC Systems

DAC Capture: The cost to capture CO₂ is technology dependent. Fasihi et al. (2019) provides cost estimates in euros per ton of CO₂. The average conversion rate in 2019 of euro to USD was used (1 EUR = 1.1201 USD) resulting in the following costs: the high temperature L-DAC technologies range from \$129 to \$435/tCO₂, the low temperature S-DAC technologies \$134 to \$273/tCO₂, and the MSA system costs about \$111/tCO₂ (Exchange-Rates).

DAC CO₂ Transportation: The main types of transportation for captured CO₂ are pipeline (onshore and offshore), truck, rail, and shipping. Fasihi et al. (2019) provides cost estimates in euros per ton of CO₂. The average conversion rate in 2019 of euro to USD (1 EUR = 1.1201 USD) was again used, along with normalizing the values based on distance. The following costs were obtained: \$0.0079 to \$0.098/tCO₂ per kilometer (km) for pipeline onshore, \$0.012 to \$0.058/tCO₂ per km for pipeline offshore, \$0.15/tCO₂ per km for trucks, \$0.014/tCO₂ per km for rail, and \$0.0068 to \$0.084/tCO₂ per km for shipping.

The choice and cost of CO₂ transportation is largely distance, terrain, and capacity dependent. For example, the cost variation with region and distances for pipelines can be viewed in Figure 2-22 (Stolaroff et al., 2021).

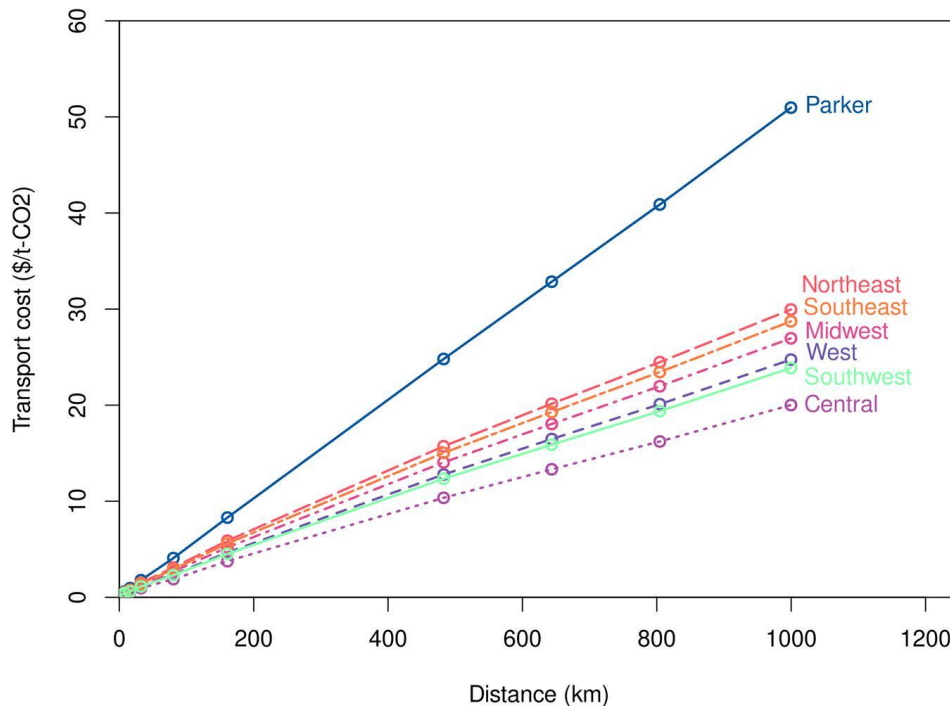


Figure 2-22: Pipeline transportation costs based on distances for regions in the U.S. using two different models: Parker (2004) and McCoy and Rubin (2008) (Stolaroff et al., 2021).

Pipelines are often favored as they are generally safer and have reduced emissions compared to other forms of transportation (Fasihi et al., 2019; Stolaroff et al., 2021).

3.0 Capacity & Cost Modeling: Powering DACs with Geothermal Energy

3.1 Model Setup

In order to assess the favorability of geothermal regions around the US to be leveraged for geothermally powered direct air capture and storage (GDACS), it is necessary to understand the amount of energy and cost required to operate GDACS facilities. To this end, a model of the energy and economics associated with potential GDACS facilities has been generated, coupled with the GeoMAP TechnoEconomic Sensitivity Tool (TEST) by project InnerSpace combined with values derived from the literature search described in the Task 1 Draft Report (TechnoEconomic Sensitivity Tool (TEST)). Both the cost and capacity are calculated assuming the geothermal source and power plant solely are powering the DAC facility, and these values are generated from publicly available literature.

The four largest contributors considered for modeling the capacity and cost of a GDACS facility are: geothermal energy production, DAC facilities, transportation of captured CO₂ to a sequestration site, and CO₂ sequestration. All four aspects must be considered collectively to determine the GDACS system's size and energy requirements. A model has been constructed that provides an estimate of the annual amount of CO₂ captured and the corresponding cost per ton of CO₂. The model considers the average net thermal energy sales from TEST. This geothermal energy estimate is applied to the DAC facility to estimate the amount of CO₂ captured per year, assuming all the geothermal electrical production is used to power the facility and that any residual heat is used to fuel the CO₂ desorption process within the DAC facility. The amount of CO₂ captured by the DAC facility is then used to calculate the cost requirements for DAC facility operation, captured CO₂ transportation and sequestration. The cost of the geothermal source and power plant is based on the CAPEX and OPEX generated by TEST.

In addition to these baseline calculations, model users are asked to provide a 'state of readiness' factor. This factor acts as an assessment of overall project risk, and accounts for unknowns and variable project costs such as exploration and appraisal drilling for geothermal and storage wells, cost to establish or repurpose existing facilities and infrastructure, and cost to manufacture new DAC technologies at scale. Users should choose their input based on their perceived level of risk of *technical* risk rather than *economic* risk.

3.2 Assumptions

Where possible, the values and assertions within this model are based on publicly available academic literature and the GEOMAP tool, as well as expert interviews conducted as part of this study. Inputs for the model are limited to the available literature and scope of the TEST tool at this time. These data may not be fully representative of the current state of the technologies in 2024, and commercial leaders in these industries most likely use their own experimentally acquired laboratory, using bench- or pilot-scale data for more accurate cost and capacity estimations. GDACS is a nascent industry with relatively few publications explicitly addressing GDACS systems and even fewer attempts by industry to build these systems. This being the case, the construction of this model necessitated that a set of baseline assumptions be made. These assumptions are as follows:

- All facilities within the model are assumed to be operational for 8,000 hours per year and represents a ~91% uptime (Fasihi et al., 2019).

- If the user does not provide a set number of geothermal production wells, the model assumes five geothermal production wells.
- The model assumes electric power plus residual heat use, since the primary purpose of the study is to determine the CO₂ capacity from the total energy of a geothermal power plant and source.
- The state of readiness defaults to three if otherwise unknown. This is the median value of the state of readiness scale and represents a project with moderate risk of technical failure.
- A 3% annual inflation rate was assumed throughout the model and all costs are scaled to 2024 costs using the following equation (Opportunity: BIL - Rare Earth Element Demonstration Facility (DE-FOA-0002618), 2022):

Equation 1:

$$\text{Current cost} = \text{Recorded cost} * 1.03^{\text{Number of years from 2024}}$$

- The DAC technology is solid sorbent based, as these systems require lower thermal requirements for desorption of CO₂.

Additional assumptions, specific to each area of the cost and capacity calculations (geothermal energy, DAC facilities, transportation, and geological storage), are given either throughout the calculations or at the end of Sections 1.3 through 1.5.

3.3 Geothermal Energy

For geothermal energy information the model user is instructed to visit the GeoMAP TEST tool (GeoMap, 2024). While using TEST the user inputs the latitude and longitude of their project and the geothermal application (power or heat in this case). The user then generates two Excel sheets by clicking “EXPORT RESULTS” for both the power application and heat application. The total CAPEX, total OPEX, average net energy sales, average net thermal energy sales, and mass flow rate per well should be taken from the TEST excel sheets and entered into the Cost & Capacity Model in the input sheet. The geothermal energy information is then used in the DAC sheet to determine DAC facility capacity and cost based on the available energy which is described in detail in Section 1.4.

3.3.1 Assumptions

GeoMAP TEST is sufficiently accurate for the cost and capacity model’s level of estimates.

4.3.2 Model Recommendations

For future iterations of this model or if additional models are constructed, the cooling of geothermal systems over time should be considered. As geothermal systems are utilized for their heat they will produce less heat. To maintain power output, additional geothermal wells may have to be drilled or the plant’s operating hours decreased. Both factors should be considered in future work. Additionally, a meeting with Project InnerSpace to walk through the cost and capacity model would be beneficial. Areas of uncertainty in GeoMAP TEST could be clearly identified so they could potentially be addressed by the model.

3.4 Direct Air Capture Facility

In this study, the modeled DAC facility is assumed to use a solid sorbent material instead of a liquid based sorbent. Solid sorbent systems tend to have desorption temperature between 80 and 130°C

(Fasihi et al., 2019; Sabatino et al., 2021), whereas liquid sorbent-based systems require much higher temperatures (about 900°C) to desorb CO₂ from the sorbents (Bertoni et al., 2024). Since the residual heat stream from geothermal power plants tends to be ~100°C, these ‘waste’ fluids can be leveraged for process heat within solid-sorbent DAC (S-DAC) technologies, where they would likely not be useful in providing process heat for liquid-sorbent systems.

User inputs to this calculation are technology readiness level (TRL), state of readiness, mass flow rate per well, average net thermal energy sales, average net energy sales, and number of production wells. The average net thermal energy sales are not used in the DAC sheet’s calculations but is there for a visual comparison for the residual heat and could be further incorporated into the model in future work.

Due to the complexity of the model calculations, the assumptions are stated within the calculation steps.

Calculation Steps

STEP 1) Estimated Capital and Operating Costs for S-DAC: In Step 1, all DAC facility components’ operating expenditures (OPEX) and capital expenditures (CAPEX) are listed in a table based on best and worst case scenarios for the market from literature (Nat.Acad. of Sci, Eng., and Med, 2019). Based on the current understanding of the DAC market, these annual costs per metric ton of CO₂ represent lower than normal estimations, which is acknowledged by the literature authors as well. The best, low and middle cost ranges are likely too optimistic; this model accounts for some of this in Step 3.

STEP 2) Unit Conversion: Step 2 converts the previous table’s CAPEX costs from a 30-year facility lifespan (assumed in the literature) to a 25-year facility lifespan to match GEOMAP’s lifespan estimation (Fasihi et al., 2019; Nat.Acad. of Sci, Eng., and Med, 2019; Opportunity: BIL - Rare Earth Element Demonstration Facility, 2022; TechnoEconomic Sensitivity Tool [TEST]). The OPEX costs remain the same as these would not be highly impacted by the facility’s lifespan.

STEP 3) Interpolation: In Step 3, a linear relationship is assumed between individual market rankings to expand the 2 (low) to 5 (worst) scale to a 1 (worst) to 9 (best) TRL (*Technology of Market*). This assumes that a higher TRL will result in better market values as the technology and engineering development will be more efficiently scaled for commercial operations. The market ranking starts at 2 (low) instead of 1 (best) to account for some of the optimistic cost range. However, this likely still provides an ideal case and is more representative of DOE’s goal of achieving \$100/tCO₂ in the future instead of a more realistic scenario (DOE, 2023).

The main OPEX that will be impacted by the residual geothermal energy is the steam OPEX. Steam is the main component of the DAC facility that is used to desorb CO₂ from the solid sorbent. Because of this, the CAPEX and OPEX are summed excluding and including the steam OPEX. The two different total costs are used later in Step 5, to calculate the cost of DAC that utilizes the residual heat and electricity for desorption.

STEP 4) Energy Requirements: Step 4 calculates the amount of energy required to release captured CO₂ from the solid sorbent. The model assumes that all captured CO₂ is released from the sorbent and that the steam OPEX is solely from the heating of the steam (as described in Step 1 of the DAC calculations). The desorption heat range is provided on a scale of 1 (lowest energy) to 4 (highest energy) with corresponding energy requirements of 1.85 GJ/tCO₂ to 1.3 GJ/tCO₂ (Nat.Acad. of Sci, Eng., and Med, 2019). This is again assumed linear between the points and it is translated to the TRL scale.

STEP 5) Residual Energy Calculations: Step 5 calculates the amount of energy that the geothermal brine provides to the DAC facility based on literature values, correction factors by subject matter experts, and GEOMAP. It is assumed that:

- The average brine temperature is 160°C.
- The outlet temperature of water from DAC facility is 40°C.
- The mass flow rate of the geothermal production well is the same as the mass flow rate into the DAC facility.
- The inlet temperature of water out of the geothermal power plant is the same inlet temperature of the fluid to the DAC facility.
- A total of 50% of the energy from the brine is lost to the surroundings during brine transfer from the power plant to the geothermal facility and during heat transfer.

Given the broad scope of these assumptions, there is a lot of room for future work which is discussed further in Chapter 4. The specific heat of brine and outlet temperature of the geothermal brine from the power plant are provided from literature. The outlet temperature is specifically from a case study of a western average sized geothermal power plant in the US (Zarriuk et al, 2014). These values are used with a standard heat transfer equation to calculate the energy per year (Equation 2).

Equation 2:

$$Q = m \times c \times \Delta T$$

where Q is the heat in kilojoules per second (KJ/s), m is the mass flow rate in kilograms per second (kg/s), c is the specific heat of brine (kJ/kg/K), ΔT is the temperature difference in Kelvin (K) between the inlet and outlet temperatures of the geothermal brine from the DAC facility.

The heat flow rate is then converted to GJ/yr and multiplied by 50% to be consistent with units in Step 6 and to account for heat loss in the heat transfer process, respectively.

STEP 6) Remaining Heat Requirements: In Step 6, the total amount of CO₂ captured per year is calculated for all nine TRL levels by using the electricity generated by the geothermal power plant as the limiting factor. The main inputs into this step are:

- **The Thermal Energy per year:** This is the heat flow rate of the geothermal brine calculated in the previous step (Step 5).
- **Average Net Energy Sales per year:** This value is calculated from GEOMAP and is input by the user in the Input sheet. The energy sale is also scaled to account for 25 years of sales and not 30 years. It was then converted from megawatts of electricity (Mwe) per year to gigajoules (GJ) per year by assuming annual 8,000 hours operations to get from MWe to MWh and then converting 1MWh to 3.5 GJ.

First the thermal energy per year is divided by the energy requirement of desorption heat per ton of CO₂ that was calculated in Step 4. This gives the tCO₂ that can be captured using the thermal energy for desorption heating. However, since this is just thermal energy that is used for desorption, the next step calculates the amount of energy it would take the DAC system to process this amount of desorbed CO₂. Thus, this amount of CO₂ is multiplied by the energy requirements for air contactor fans and desorption fans to find the remaining energy needed. The next step subtracts the average net energy sales per year by the energy needed for air contractor and desorption fans to find the remaining energy

available. The remaining energy available is the limiting factor of this model. The remaining energy available is then divided by the total energy requirements for each TRL level to calculate the additional tCO₂ that can be captured by the DAC facility.

The total tCO₂ sums the tCO₂ captured with remaining energy and tCO₂ captured from thermal energy if the remaining energy available is above zero gigajoules electricity (GJe). Otherwise, the total tCO₂ captured is the average net energy sales divided by the total energy requirements for the DAC system.

Lastly, for each TRL if the remaining energy available is above 0 GJe, the annual cost of the facility is calculated by multiplying the tCO₂ from thermal energy used for desorption heating by the total cost of the DAC facility without steam. This is summed with the product of the tCO₂ captured with remaining energy and the total cost of the DAC facility per tCO₂ with steam that was calculated in Step 3. Otherwise, the annual cost of the facility is just the product of the tCO₂ captured with remaining energy and the total cost of the DAC facility per tCO₂ with steam that was calculated in Step 3.

Results: The annual tCO₂ captured, annual cost of facility, and cost per tCO₂ are shown in the results section and are all output to the Overall Costs sheet. The Annual tCO₂ Captured is also sent to the Transportation and Storage sheets.

3.4.1 Model Recommendations

For future iterations of this model, or if additional models are constructed, liquid sorbents and process heat losses should be considered. The liquid sorbent calculation would follow a similar method as the solid sorbent method but likely would need much higher heating requirements. This may result in much higher energy costs that may or may not be attainable with a geothermal power facility. Accounting for heat loss in the process would likely entail the losses during transportation of the geothermal source from the power plant or reservoir to the DAC facility. Additional inefficiencies within the DAC facility could be considered by taking into account variables like sorbent material, surface air, and local climate.

The residual heat (Step 5) calculation also would be an excellent candidate for future work. The efficiency of power plants is highly dependent on factors such as power plant type, for example single flash, double flash, and binary plants. Thus, a range of efficiencies or a more accurate efficiency could be provided for models.

3.5 Transportation

3.5.1 Transportation Calculations

The transportation cost calculations start with four inputs: type of CO₂ transportation, storage distance from capture (km), state of readiness, and annual tCO₂ captured.

Calculation Steps

STEP 1a) Cost Based on Type and Year: Five types of transportation were considered for this model: pipeline on and off shore, truck, rail, and barge. A table based on literature values provided ranges of costs for each transportation type that was published in Fasihi et al. (2019). These costs were adjusted for inflation to 2024 values based off the citation years within Fasihi et al. (2019). The costs are also originally in euros, so the average exchange rate from the citation year is used to convert the costs to dollars. The costs per tCO₂ are then divided by the corresponding distances given in the table to get the

units as \$/tCO₂ per km. The minimum and maximum costs for each transportation type are identified to be used in the model.

STEP 1b) Transportation Cost Summary: Step 1b summarizes the calculations from Step 1a for each transportation type.

STEP 2) Cost Based Distance: In Step 2, the 2024 cost range is multiplied by the distance traveled to give a cost range in \$/tCO₂. The state of readiness is applied.

STEP 3) Annual Costs: In Step 3, the cost ranges calculated in Step 2 are multiplied by the amount of CO₂ that is captured to yield the overall costs per year.

Results: The annual minimum, maximum and with state of readiness transportation costs are in the Results section. These all are output to the Overall Costs sheet.

3.5.2 Assumptions

If the user inputs unknown or other for the type of captured CO₂ transportation, an onshore pipeline is assumed because of their associated safety precautions and regulations (Fasihi et al., 2019; Stolaroff et al., 2021). If the user inputs unknown for the storage distance from capture, 25 km is used as a default.

3.5.3 Model Recommendations

In the future, regional and terrain specific considerations such as elevation gain, gas pricing, and established infrastructure would be beneficial to provide a more accurate cost estimate. For example, if pipelines already exist, the initial upfront cost would be reduced. Also, future work should consider specific cost breakdowns that show how factors like compressing CO₂ for transportation impact the costs.

3.6 Geological Storage

The geological storage calculations start with two inputs: state of readiness and annual tCO₂ captured.

3.6.1 Storage Calculations

STEP 1) Injection, Monitoring, and Verification Costs: In Step 1 on the Storage Costs sheet, injection, monitoring, and verification costs were gathered from the Global CCS Institute (2021) and adjusted for inflation to 2024 prices (*Opportunity: BIL - Rare Earth Element Demonstration Facility*, 2022). The cost of injection per tonnes of CO₂ includes drilling wells, reservoir characterization, and injection operations.

STEP 2) Unit Conversion: The annual amount of CO₂ captured is multiplied by the total costs calculated in Step 1 to determine the annual costs. The minimum, maximum, and the state of readiness costs are separately summed for the total cost range.

Results: The minimum, maximum and state of readiness annual storage costs are output to the Overall Costs sheet.

3.6.2 Assumptions

For the geological storage calculations, it is assumed that the geological storage is not the limiting factor of this model. Instead, the geothermal source and DAC facility would limit the CO₂ capture

capacity. Also, it is assumed that all the CO₂ captured by the DAC facility is successfully transported and sequestered with no losses.

4.0 Uncertainties and Recommendations for Future Work

This section details the uncertainties remaining for these systems, including geological and technological uncertainties, and may include regulatory, cost, and operational uncertainties. Recommendations for future work will also be provided to continue de-risking these systems and optimizing the selection of locations for geothermally powered DAC + storage.

4.1 Uncertainties in geothermal energy development

The vast majority of existing geothermal power in the United States comes from hydrothermal developments. However, the bulk of likely geothermal development between now and 2050 is expected to utilize EGS or closed-loop technologies. While significant advancements in drilling techniques, well stimulation, and fluid and heat flow modeling have moved these technologies into active development, the long-term performance of these play styles is still unknown. Additionally, there are non-technical issues, such as the state-by-state patchwork of regulatory standards, community and environmental justice issues (particularly around water usage in arid western states), and public acceptance that may hamper permitting and project development, potentially resulting in significant delays to bringing new capacity online.

4.2 Uncertainties in carbon storage development

The fundamentals of carbon storage, both in saline aquifers and in depleted petroleum reservoirs, is relatively well understood. Projects around the globe have successfully injected and contained CO₂ in both play styles and the progression of permitting, appraisal, and development is accelerating across the country. However, basalt formations have received considerably less study and there is significant uncertainty as to their accept and store significant quantities of CO₂ over the long term. Continued appraisal is needed to drive development in all play styles, but significantly more study is needed to derisk the potential for basalt storage in terrains where these may be the only available storage targets.

Many carbon storage projects deal with uncertainty as to permitting and development timelines, as a result community acceptance, particularly when it comes to siting surface facilities and construction of CO₂ transmission pipelines. Community and environmental justice are critical aspects of ethical and effective carbon storage development, and continued focus on public education, outreach, and community engagement will be critical to reducing project risk and uncertainty over the coming years.

4.3 Uncertainties in DAC development

It is still unclear whether solid sorbent systems or liquid sorbent systems will ultimately be the most efficient, and each may have applications depending on the available power source. Solid sorbent systems have lower energy input than liquid systems but have more complex technology requirements when releasing the captured CO₂ from their sorbent (e.g. mobile units to create vacuums and change temperatures to release CO₂ from sorbent). The type of system can be further broken down into factors such as alkali vs amine-based solvents or sorbent type. These can all impact what technology will scale the best. Economic sustainability is also a concern for DAC technologies, as operational costs are likely to vary significantly between technologies over their operations lifespans. There is also uncertainty in the volume and stability of carbon credit markets, with prices and customer volumes likely dependent on a number of factors that may vary results in significant volatility over time.

4.4 Uncertainties in GDACS development

Given that each element of the GDACS process carries its own unique uncertainties, and since all elements of a GDACS project must be successful for the project to succeed, it is clear that GDACS projects will carry significant uncertainty and significant risk. These uncertainties can likely be reduced by carefully siting geothermal and storage facilities within well-established plays and using DAC technologies that are operationally simple. Risk may also be reduced by coupling GDACS projects with geothermal and carbon storage developments that have other clients, thereby spreading operational and economic risk among multiple parties.

4.5. Uncertainties in the GDACS Cost and Capacity Model

4.5.1 Global model uncertainties

The Project InnerSpace GeoMap™ was developed by an organization outside of USEA and Battelle and is not associated with this study

Due to the Cost and Capacity Model relying on data input from the GeoMap™ tool, there is a level of uncertainty associated with the data. Neither Battelle nor USEA had any influence or input on Project InnerSpace's processes to develop the tool, which may lead to discrepancies, such as data collection processes, analysis assumptions, and optimization factors. This tool is also directed towards enhanced geothermal systems, so production and economic values that are derived from the tool may not be reliable where the primary play style is not EGS. Additionally, the GeoMap™ tool provides high-level, regional or fairway-scale analysis. Values derived from the tool such as geothermal gradient, drilling depth, and flow rates may overrepresent or underrepresent the true values achievable at any given location, and, as such, should be treated as a guide rather than a ground truth. The current known assumptions are available in GeoMap™ user guides at the following website: [GeoMap™ Beta | Project InnerSpace](#)

State of Readiness Scale

The state of readiness is a user defined input that allows the model to narrow ranges of costs based on a 5-point scale (1 being the best and 5 being the worst). The 5-point scale is based on literature values that use 5-point ranking systems (Nat.Acad. of Sci, Eng., and Med, 2019; Kuru et al, 2023). This scale was developed for the model to account for different situations that would impact the cost and capacity of the geothermally powered DAC facility such as established infrastructure and knowledge base.

4.5.2. DAC model uncertainties

Model estimated capital and operating costs appear low (Step 1).

The DAC model estimated capital and operating costs appear to be too low (Step 1). Literature values estimate the range of annual costs for the solid DAC systems from \$18.03 to \$1,075.50 per Mt of CO₂. These costs depend on factors such as TRL and the state of the economy. The lower end of the cost range would likely have a TRL of 9 and the facility would operate likely in an idealized economy. However, the U.S. DOE's stated goal of is to reach \$100 per tCO₂ (DOE Invests More Than \$130 Million to Lower Nation's Carbon Pollution, 2023). Thus, the model was adjusted to count a TRL of 9 as

a cost level of 2, which assumes the lowest cost is \$102.37 per tCO₂. This cost estimate is still optimistic and represents a stretch goal with new or developing technology. There is still significant uncertainty around DAC capital and operating costs at scale, especially those associated with higher TRLs.

Model scales cost and energy demands to TRL and assumes linear relationships between levels (Steps 3 and 4).

Our model assumes that better technology (a higher TRL) will result in better market values and energy efficiencies. This assumption directly impacts Step 3 with CAPEX and OPEX costs and Step 4 with heat and energy requirements. A linear relationship was assumed for cost and energy levels. The linear relationship allows for a smooth translation from a cost scale of 1 to 5 and an energy scale of 1 to 4 to the TRL scale of 1 to 9. Thus, there is some uncertainty about the accuracy of the TRL's relationship with cost and energy.

Residual energy calculation and power plant variability (Step 4).

The residual energy calculation uses a standard heat transfer equation. The specific heat of brine and inlet temperature from DAC are literature values. It is assumed that the inlet temperature at the DAC facility is identical to the outlet temperature of the geothermal power plant. This does not account for heat loss between the Geothermal Power plant and the DAC facility. The literature values are also derived from a single paper (Zarrouk et al, 2014). This paper provides a list of case studies on different plants, with values selected from a typical geothermal power plant in the western region of the US. In reality, power plant outputs differ greatly depending on factors such as the type of power plant, utilization of waste heat, and facility efficiency. Also, the specific heat of brine is highly dependent on brine composition, which can vary widely from location to location.

Additionally, the mass flow rate of the brine from the geothermal power plant to the DAC facility is assumed to be the mass flow rate of the well. In actuality, this will also depend on the equipment (e.g. pipe dimensions, pumps, flow lengths) in both the DAC facility and geothermal power plant. To account for heat loss through the heat transfer process from the DAC facility to the geothermal facility a board assumption of 50% energy loss was used. However, this is also dependent on many factors such as heat transfer equipment (size, efficiency, type). Thus, there is much uncertainty in this part of the model.

Limiting Factor in CO₂ capture (Step 5).

This model assumes all the electrical power generated by the geothermal power plant directly feeds into the DAC facility. The model uses the generated electrical power and associated geothermal heat as the limiting factors for the amount of CO₂ that can be captured. There are likely other factors that could limit the amount of CO₂ captured at specific sites, such as cooling of geothermal resources and the injection rate or storage capacity of associated carbon sequestration targets.

Operation of Facilities (Step 5).

The model assumes that both the geothermal power plant and DAC facility operate for 8,000 hours per year (approximately 333 days per year or 91% uptime). This assumption is based on a rare earth element demonstration facility from the DOE (Opportunity: BIL - Rare Earth Element Demonstration Facility) and may differ from actual geothermal power plant and DAC facility uptimes. Also, the

geothermal power plant and DAC facility may differ in operational hours from each other. Furthermore, the model does not account for the geothermal resource cooling over time, which may reduce operational uptime in the later years of the project.

Geothermal Source

Geothermal sources typically cool over time. The sources have a lifespan that may not meet the power plant or DAC facility production requirements. In turn, the facilities may have to draw on multiple geothermal sources or decrease the scale of operation. While geothermal power decline curves are accounted for in the GeoMap™ TechnoEconomic Sensitivity Tool that the model relies on, these variables are not considered directly in the model and can be highly variable depending on both the geothermal energy source and facility design, which introduces uncertainty in the cost and capacity estimations.

4.5.3 Transportation model uncertainties

Cost Ranges

Cost estimates for transportation were taken from literature and were from three different years and listed in euros. The average exchange rate of each source's year was used to convert the units from euros to U.S. dollars and then an average inflation rate of 3% was assumed. A cost range was used for pipeline onshore, pipeline offshore, and barge costs. However, transportation via truck and rail each had a single cost listed in the literature, thus no range was available. These assumptions all contribute to uncertainty in the transportation cost calculation.

Transportation and storage energy

Energy used for transportation is not addressed in the model. In most cases, energy would be used to compress CO₂ to the liquid state for transportation via trucks, barges, and rail, and to a supercritical state for transportation via pipeline. This energy would likely come from the electrical output of the geothermal power plant, reducing the energy available for DAC. Additional energy may also be required from the power plant in the case of pipeline transportation in order to account for energy use of the pipeline itself. In areas where the geothermal power plant and storage facility are either co-located or proximal to each other, additional power may be used to power the storage facility, again reducing the energy available for DAC.

4.5.4 Storage model uncertainties

Combined Costs

The storage cost calculation uses two cost ranges from literature: one for injection costs and one for monitoring and verification costs. The injection cost range includes drilling reservoir characterization wells, injection wells, and injection operations. However, these costs can be highly variable depending on factors such as reservoir depth, site exploration and characterization costs, availability of infrastructure, number of storage wells required, and storage formation injectivity and capacity.

4.6 Recommendations for Future Models:

4.6.1. Global Recommendations

Expand inclusion of literature, case studies, and FEED studies.

Our cost and capacity model is primarily based on available public literature. Some of the key aspects of geothermal, DAC, and carbon storage systems are still in the early phases of study, so at the time of writing, many of the relevant variables are represented by few sources and large error bars. As such, some estimations and calculations are based on a single paper or study. Future researchers may be able to draw upon a broader pool of papers, industry data, and front-end engineering and design (FEED) studies to increase the reliability, accuracy, and precision of the model.

Utilize additional software.

This model draws upon the Project InnerSpace GeoMap™ tool for variables associated with geothermal energy production. The model could be easily adapted to receive inputs from other tools or software that specialize in specific components of the model. To assess pipeline transportation distances associated with our example prospects, SimCCS, a pipeline modeling software that was developed by Los Alamos National Laboratory that takes into account factors such as land use restrictions and environmental and social justice components to determine optimal pipeline routes between GDAC facilities and storage locations, was employed. However, cost from SimCCS was not incorporated into the model. Future iterations of the model should integrate SimCCS outputs into the transportation section of the model. Another tool that could be beneficial for assessing CO₂ transportation costs is the DOE National Energy Technology Lab (NETL) CO₂ Transport Cost Model (DOE/NETL-2014/1667). This tool utilizes factors such as pipeline elevation change and length to provide the user with cost estimates and pipeline details such as number of booster pumps and pipeline diameter, which may allow future models to include both the costs and power needs of the transportation portion of the system. Inputs from tools such as the NETL CO₂-SCREEN tool can provide estimates of CO₂ storage volumes and footprints for targeted storage locations.

Breakdown of costs.

The overall costs of geothermal, DAC, and injection systems are handled at a relatively high level in this model. There is room for future models to be more granular in their assessment of operating and maintenance costs. The annualized costs currently can provide additional insight into the general areas (DAC, geothermal, transportation) in need of further cost reduction or improved efficiencies. However, these areas could be further refined into sections such as solid sorbent or liquid solvent costs of DAC facilities or cost of fuel for trucks or cost of heat exchangers for the geothermal power plant. This would provide the user with transparency in terms of the costs and supply potential areas for optimization efforts.

4.6.2. Geothermal Power Model Recommendations

Include detailed estimates of cost and power output for hydrothermal systems, advanced geothermal systems, and sedimentary geothermal systems.

The GeoMap™ tool is aimed primarily at showcasing the broad application of enhanced geothermal systems around the world. Because of the limited scope of this study and the likely prevalence of

enhanced geothermal development over the coming decades, GeoMap's power outputs and cost estimates were leveraged in this model. Future models should build in flexibility when it comes to the style of geothermal development being utilized for power, as hydrothermal systems, AGS, and sedimentary geothermal all have potential to be included in GDACS developments and have substantial differences in power production profiles and development and operational costs.

Include estimates of subsurface geothermal development footprint

The GeoMap™ tool provides estimates of the geothermal power capacity of developments across geographic and geological regions, and provides an estimate of the surface footprint necessary for geothermal development. However, it does not provide an estimate of the subsurface footprint of those developments. Future models could incorporate estimates of stimulated or exploited reservoir volume on a per-well basis to provide model users with an approximate footprint for their geothermal development.

4.6.3. DAC Model Recommendations

Capital and Operating Costs (Step 1).

We recommend that future efforts utilize additional literature, software, and more granular cost breakdowns as mentioned in Section 4.5.1. However, if a specific cost breakdown is not possible, specific costs could be divided by overall costs to calculate a ratio. This ratio could be applied to overall costs found in literature to estimate a more comprehensive list of expenses. For example, the vacuum pump CAPEX could be divided by the overall total costs of the DAC facility to see what ratio of the total cost the vacuum pump consumes. This ratio could be used to estimate the vacuum pump CAPEX of a DAC facility that only has a total cost available, not a breakdown of the CAPEX and OPEX numbers.

Residual energy calculation and power plant variability (Step 4).

Adding a section of the model dedicated to residual energy availability and power plant variability is recommended. Tools should be utilized for heat transfer in power plants, break down calculations based on power plant types, efficiency, size and capacity of the power plant, equipment, and length of transportation of the geothermal brine. Calculations of specific heat based on brine density or composition should be included. Mass flow rates should be based on known or expected waste stream outputs of geothermal power plants and not on the mass flow rate of the geothermal wells.

Limiting factors.

Consider other limiting factors besides generated electrical power and the geothermal heat:

- The geothermal source could be directly used by the DAC facility for heat exchange and an external energy source could be used.
- The residual heat from the geothermal power plant could capture CO₂ and the remaining energy sold commercially.

In this broad, regional and fairway-scale study, it was assumed that the GDACS facility had access to storage volumes that are greater than the output of the DAC facility. Future models could consider the storage capacity or maximum injection rate of the CO₂ storage facility as a limiting factor. This may impact the amount of CO₂ that can be captured or that is economically viable.

Consider additional DAC technologies.

The current model only evaluates solid sorbent DAC technology, as these technologies tend to require the lowest temperatures. Future models could be expanded to evaluate the capabilities of DAC facilities utilizing liquid sorbent technologies.

Include broader market and economic analysis.

This model only evaluates the cost of constructing and operating GDACS facilities at a relatively high level. Future models could expand on this analysis, providing more granular cost estimates for each part of the process. Future models could also include economic analysis that takes into account tax credits, such as 45Q as well, as options for selling carbon credits on the voluntary market.

4.6.4. Transportation Model Recommendations

Include pipeline energy and equipment requirements to inform cost and impact on DAC facility output.

Future models should incorporate pipeline size, energy requirements, and detailed costs for CO₂ transportation from the DAC facility to the storage facility, based on estimated distance, estimated CO₂ volume, and predicted pipeline equipment specifications. This will add significant resolution both to the cost model and to the capacity of the total system to capture CO₂, as noted above.

4.6.5. Storage Model Recommendations

Include storage volume estimation (MT/km²) as input in model to provide plume diameter estimate.

Understanding the subsurface footprint of a planned carbon storage development is a key factor in siting the facility correctly, planning appropriate appraisal, injection, and monitoring well drilling, and informing the plume monitoring strategy. Future models could address carbon storage footprints in at least two different ways:

1. Building in a set of basic volumetric calculations that allow users to enter values from their reservoir analysis and output simple results for storage volume per square kilometer and approximate CO₂ plume diameter. This would be quick and simple, but would carry relatively high uncertainty.
2. Building in results from a tool such as the NETL's CO₂-SCREEN as mentioned above, which would provide a significantly higher resolution understanding of plume diameter, but likely also requires a relatively high level of information about the targeted storage system.

Build in variable cost for carbon storage characterization and development wells and monitoring and verification systems.

A key driver for the economics of carbon storage developments is the upfront cost of appraisal, injection, and monitoring wells and other elements of the monitoring and verification system. These costs are directly related to the style of carbon storage play being targeted (saline storage versus depleted reservoir storage versus basalt storage), the depth of the storage target, reservoir quality, the estimated radius of the CO₂ plume, and a number of other factors. The model assumes that storage costs scale directly with annual injected volumes, but this is likely not the case for every development.

4.0 Uncertainties and Recommendations for Future Work

Future models should build in variables that can account for these costs to provide a clearer picture of the CAPEX and OPEX profiles for the storage component of the GDACS system.

5.0 References

- Abdulagatov, I.M., Emirov, S.N., Abdulagatova, Z.Z., Askerov, S.Y., 2006, Effect of Pressure and Temperature on the Thermal Conductivity of Rocks, *Journal of Chemical Engineering Data*, No 51, P. 22-33.
- Ajayi, T., Gomes, J. S., & Bera, A. (2019). A review of CO₂ storage in geological formations emphasizing modeling, monitoring and capacity estimation approaches. *Petroleum Science*, 16, 1028–1063. <https://doi.org/10.1007/s12182-019-0340-8>
- Alonzo. C., Larry Boudreau, Kellie Cross, Jeffery Keevan, Bryan Stephens, Shane Stradley, Kevin Trosclair. (2022). Identification of Tier 1 Depleted Reservoirs in the
- Augustine, Chad, Sarah Fisher, Jonathan Ho, Ian Warren, and Erik Witter. 2023. Enhanced Geothermal Shot Analysis for the Geothermal Technologies Office. Golden, CO: National Renewable Energy Laboratory. NREL/TP-5700-84822. <https://www.nrel.gov/docs/fy23osti/84822.pdf>.
- Bachu, S. (2003). Sequestration of CO₂ in geological media in response to climate change: Capacity of deep saline aquifers to sequester CO₂ in solution. *Energy Conversion and Management*, 44(20), 3151-3175.
- Bachu, S. (2008). CO₂ storage in geological media: Role, means, status and barriers to deployment. *Progress in Energy and Combustion Science*, 34(2), 254-273.
- Backus, G.E., 1975, Gross Thermodynamics of Heat Engines in Deep Interior of Earth, *Proceedings of the National Academy of Sciences, United States of America*, V. 72, No. 4, pp 1555-1558.
- Bauer, M. (2012). Assessment of the potential for carbon dioxide sequestration in the Appalachian Basin and the western portion of the Appalachian Plateau. U.S. Department of Energy, National Energy Technology Laboratory.
- Benson, S. M., & Orr, F. M. Jr. (2016). *Carbon Dioxide Capture and Storage*. Stanford University, USA.
- Bertoni, L., Roussanaly S., Riboldi L., Anantharaman R., & Gazzani, M. (2024). Integrating direct air capture with small modular nuclear reactors: understanding performance, cost, and potential. *Journal of Physics: Energy*, (6) 025004.
- Birdsell, D.T., Adams, B.M., Deb, P., Ogland-Hand, J.D., Bielicki, J.M., Flemming, M.R., Saar, M.O., 2024, Analytical solutions to evaluate the geothermal energy generation potential from sedimentary-basin reservoirs, *Geothermics*, Volume 116, 2024, 102843,ISSN 0375-6505, <https://doi.org/10.1016/j.geothermics.2023.102843>.
- Blankenship, D., Gertler, C., Kamaludeen, M., O'Connor, M., & Porse, S. (2024). Pathways to Commercial Liftoff: Next-Generation Geothermal Power. Geothermal Technologies Office.
- Bradshaw, J., & Bachu, S. (2016). A review of risks and uncertainties associated with CO₂ storage. *Advances in CO₂ Capture, Sequestration, and Conversion*, 43-74.
- Buursink, M. L., Merrill, M., Craddock, W. H., Roberts-Ashby, T. L., Brennan, S. T., Blondes, M. S., ... & Lohr, C. D. (2014). Geologic Framework for the National Assessment of Carbon Dioxide Storage Resources: Williston Basin, Central Montana Basins, and Montana Thrust Belt Study Areas: In *Geologic Framework for the National Assessment of Carbon Dioxide Storage Resources*. Chapter J. US Department of the Interior, US Geological Survey.

- Buursink, M.L., Slucher, E.R., Brennan, S.T., Doolan, C.A., Drake, R.M., II, Merrill, M.D., Warwick, P.D., Blondes, M.S., Freeman, P.A., Cahan, S.M., DeVera, C.A., and Lohr, C.D., 2014, Geologic framework for the national assessment of carbon dioxide storage resources—Greater Green River Basin, Wyoming, Colorado, and Utah, and Wyoming-Idaho-Utah Thrust Belt, chap. E of Warwick, P.D., and Corum, M.D., eds., Geologic framework for the national assessment of carbon dioxide storage resources: U.S. Geological Survey Open-File Report 2012–1024–E, 50 p., <http://dx.doi.org/10.3133/ofr20121024E>.
- Cao, R., Miller, Q. R.S., Davidson, C.L., Gallin, W., Reidel, S. P., Jiao, Z., McLaughlin, J.F., Nienhuis, E.T., Schaef, H.T., Gigaton commercial-scale carbon storage and mineralization potential in stacked Columbia River basalt reservoirs, *International Journal of Greenhouse Gas Control*, Volume 137, 2024, 104206, ISSN 1750-5836, <https://doi.org/10.1016/j.ijggc.2024.104206>.
- Carbon Storage FAQs. (2024). Illustration of Pressure Effects on CO₂ (based upon image from CO2CRC). Retrieved from <https://www.netl.doe.gov/carbon-management/carbon-storage/faqs/carbon-storage-faqs>
- Congressional Budget Office. (2023). Report Title. <https://www.cbo.gov/publication/59832> (2024).
- Cottrell, M., Lacazette, A., Chmela, B., Karimi, S., & Marsh, B. D. (2023, June). Evaluating the Geothermal Potential of Hot Sedimentary Aquifers Using a Hybrid Approach. In *ARMA US Rock Mechanics/Geomechanics Symposium* (pp. ARMA-2023). ARMA.
- DOE, Office of Fossil Energy and Carbon Management (FECM). (2022). Strategic Vision – The Role of Fossil Energy and Carbon Management in Achieving Net-Zero Greenhouse Gas Emissions. 75 p.
- DOE, 2023, DOE Invests More Than \$130 Million to Lower Nation’s Carbon Pollution, website. <https://www.energy.gov/articles/doe-invests-more-130-million-lower-nations-carbon-pollution#>
- Downey, Cameron, & Clinkenbeard, John. *An Overview of Geologic Carbon Sequestration Potential in California*. United States. <https://doi.org/10.2172/903323>
- Exchange-Rates. Euro (EUR) To US Dollar (USD) Exchange Rate History for 2019. EUR to USD Exchange Rate History for 2019 (exchange-rates.org). Accessed 11 Apr. 2024
- Fasihi, M., Efimova, O., & Breyer, C. (2019). Techno-economic assessment of CO₂ direct air capture plants. *Journal of Cleaner Production*, (224), 957-980.
- Faulds, J.E., et al. (2011). Geothermal Play Fairway Analysis of the Great Basin. Nevada Bureau of Mines and Geology.
- Faulds, J. E., & Hinz, N. H. (2015). "Favorable Tectonic and Structural Settings of Geothermal Systems in the Great Basin Region, Western USA: Proxies for Discovering Blind Geothermal Systems." Nevada Bureau of Mines and Geology, University of Nevada, Reno, NV 89557. Email: jfaulds@unr.edu.
- Fernández, L. (2024). U.S. geothermal power plants 2021, by state. Number of geothermal power plants in the United States as of 2021, by state. Statista. <https://www.statista.com/statistics/749659/us-geothermal-power-plants-by-state/>
- Forson, Corina, Swyer, Michael W., Schmalzle, Gina M., Czajkowski, Jessica L., Cladouhos, Trenton T., Davatzes, Nicholas, Norman, David K., and Cole, Ryan A. *Geothermal play-fairway analysis of Washington State prospects*. United States: N. p., 2015. Web.

Frash, L. P., Iyare, U. C., KC, B., Meng, M., Smith, M., & Kroll, K. (2024, June). High Temperature Triaxial Direct-Shear Testing for FORGE and Field Scale Implications. In *ARMA US Rock Mechanics/Geomechanics Symposium* (p. D042S059R005). ARMA.

GeoMap, Project InnerSpace, 2024, <https://geomap.projectinnerspace.org/geomap/> or <https://geomap.projectinnerspace.org/map-selection/>

Global CCS Institute. (2021). Technology Readiness and Costs of CCS. Dr. David Kearns, Senior Consultant, CCS Technology; Dr. Harry Liu, Consultant, CCS Projects; Dr. Chris Consoli, Senior Consultant, Storage.

Godec, M., Koperna, G., Petrusak, R. and Oudinot, A. (2013). Potential for enhanced gas recovery and CO₂ storage in the Marcellus Shale in the Eastern United States. *International Journal of Coal Geology*, 118, pp.95-104.

Goff, F., Grigsby, C.O., 1982, Valles Caldera geothermal systems, New Mexico, U.S.A., *Journal of Hydrology*, Volume 56, Issues 1–2, P. 119-136, ISSN 0022-1694, [https://doi.org/10.1016/0022-1694\(82\)90061-0](https://doi.org/10.1016/0022-1694(82)90061-0).

Goldberg, D. (2018). Carbon sequestration in the Pacific Northwest. U.S. Geological Survey.

Goldberg, D. S., Kent, D. B., & Balashov, V. N. (2008). Rapid, high-temperature, pressure-induced mineral carbonation of CO₂-rich flue gas: A review of containment and resource implications. *International Journal of Greenhouse Gas Control*, 2(1), 112-120.

Goldberg, D. S., Lackner, K. S., Han, P., Lomax, J., & Tanaka, M. (2008). Making CO₂ storage work: Challenges and opportunities for the petroleum and geosystems engineering community. *SPE Journal*, 13(03), 352-364.

Gosnold, W., Abdureyimu, S., Tsiryapkina, I., Wang, D., Ballesteros, M., Geothermal and Electric Power Analysis of Horizontal Oil Well Fields, Williston Basin, North Dakota, USA, Conference, AAPG European Region, 3rd Hydrocarbon Geothermal Cross Over Technology Workshop, Geneva, Switzerland, April 9-10, 2019, DOI: 10.1306/80681Gosnold2019

Gulf of Mexico, SECARB Offshore – GoMCarb Gulf of Mexico Annual Joint Partnership Meeting, BOEM. <https://www.boem.gov/about-boem/regulations-guidance/carbon-sequestration>

Gupta, H., Roy, S., Chapter 4 - GEOTHERMAL SYSTEMS AND RESOURCES, Editor(s): Harsh Gupta, Sukanta Roy, Geothermal Energy, Elsevier, 2007, Pages 49-59, ISBN 9780444528759, <https://doi.org/10.1016/B978-044452875-9/50004-6>.

Gupta, N., Paul, D., Cumming, L., Place, M., & Mannes, R. G. (2014). Testing for large-scale CO₂-enhanced oil recovery and geologic storage in the Midwestern USA. *Energy Procedia*, 63, 6393-6403.

IEA, Energy needs of L-DAC and S-DAC, 2023, IEA, Paris <https://www.iea.org/data-and-statistics/charts/energy-needs-of-l-dac-and-s-dac-2023>, IEA. License: CC BY 4.0

IEA, 2020. Special Report on Carbon Capture Utilisation and Storage: CCUS in Clean Energy Transitions. International Energy Agency. Retrieved from <https://www.iea.org>

IEA Greenhouse Gas R&D Programme (IEA GHG), “CCS Site Characterisation Criteria”, 2009/10, July 2009.

Ingebritsen, S. E., & Manning, C. E. (2010). Geothermal systems and energy resources: Heat, fluids, and tectonics. American Geophysical Union.

Ingebritsen, S. E., & Wannamaker, P. E. (2017). Geothermal systems and tectonics: A tale of two theories. *Geosphere*, 13(6), 1-26.

IPCC, 2022: Climate Change 2022: Mitigation of Climate Change. Contribution of Working Group III to the Sixth Assessment Report of the Intergovernmental Panel on Climate Change [P.R. Shukla, J. Skea, R. Slade, A. Al Khourdajie, R. van Diemen, D. McCollum, M. Pathak, S. Some, P. Vyas, R. Fradera, M. Belkacemi, A. Hasija, G. Lisboa, S. Luz, J. Malley, (eds.)]. Cambridge University Press, Cambridge, UK and New York, NY, USA. doi: 10.1017/9781009157926

Jones, C., Moore, J., Teplow, W., Craig, S., 2011, Geology and Hydrothermal Alteration of the Raft River Geothermal System, Idaho. Proceedings, Thirty-Sixth Workshop on Geothermal Reservoir Engineering, Stanford University, Stanford, California, January 31 - February 2, 2011, <https://pangea.stanford.edu/ERE/pdf/IGAstandard/SGW/2011/jones.pdf>

Kang, S. M., E. Fathi, R. Ambrose, I. Akkutlu, and R. Sigal, 2011, Carbon dioxide storage capacity of organic-rich shales: *SPE Journal*, v. 16, p. 842–855

Khodayar, M. and Björnsson, S. (2024) Conventional Geothermal Systems and Unconventional Geothermal Developments: An Overview. *Open Journal of Geology*, 14, 196-246. doi: 10.4236/ojg.2024.142012

Kuru, T., Khaleghi, K., & Livescu, S. (2023). Solid sorbent direct air capture using geothermal energy resources (S-DAC-GT) – Region specific analysis. *Geoenergy Science and Engineering*, (224). 211645.

Lacazette, A., Cumella, S. P., Matt, V. J., Cottrell, M. G., Karimi, S., Marsh, B. D., & Chmela, W. R. 2024, Using Petroleum Industry Data to Locate, Characterize, and Simulate a Hot Sedimentary Aquifer Geothermal Prospect. Proceedings, 49th Workshop on Geothermal Reservoir Engineering, Stanford University, Stanford, California, February 12-14, 2024

Lazard. (2023). Levelized Cost Of Energy+. Reports and Studies — Financial Advisory, Levelized Cost of Energy, Levelized Cost of Hydrogen, Levelized Cost of Storage, LCOE. <https://www.lazard.com/research-insights/2023-levelized-cost-of-energyplus/>

Lund, J. W., & Boyd, T. L. (2016). Direct utilization of geothermal energy 2015 worldwide review. *Geothermics*, 60, 66-93.

Mccleery, R.S., McDowell, R.R., Moore, J.P., Garapati, N., Carr, T.R., Anderson, B.J., 2018, Development of 3-D Geological Model of Tuscarora Sandstone for Feasibility of Deep Direct-Use Geothermal at West Virginia University’s Main Campus, *GRC Transactions*, Vol. 42, 2018, https://qdr.openei.org/files/1097/GRC_2018_RevisedPaper_WVU.pdf

McCoy, S. T., & Rubin, E. S. (2008). An engineering-economic model of pipeline transport of CO₂ with application to carbon capture and storage. *International Journal of Greenhouse Gas Control*, 2(2), 219-229.

McGrail, B.P., Spane, F.A., Sullivan, E.C., Bacon, D.H., Hund, G., The Wallula basalt sequestration pilot project, *Energy Procedia*, Volume 4, 2011, Pages 5653-5660, ISSN 1876-6102, <https://doi.org/10.1016/j.egypro.2011.02.557>.

- McPherson, B. J. O., Cantrell, D., & Sherk, G. W. (2005). Carbon dioxide enhanced oil recovery—A critical component of a national greenhouse gas strategy. *Oil & Gas Journal*, 103(40), 32-39.
- Michael, K., Golab, A. N., Shulakova, V., Aiken, T., et al. (July 2010). Geological storage of CO₂ in saline aquifers--A review of the experience from existing storage operations. *International Journal of Greenhouse Gas Control*, In Press, Corrected Proof. DOI: 10.1016/j.ijggc.2009.12.011.
- Morgan, P. (2017). Geothermal Power Generation in the Rocky Mountain States: An Overview. *Energy Sources, Part A: Recovery, Utilization, and Environmental Effects*, 39(3), 307-314.
- Mostafa, M., Antonicelli, C., Varela, C., Barletta, D., & Zondervan, E. (2022). Capturing CO₂ from the atmosphere: Design and analysis of a large-scale DAC facility. *Carbon Capture Science & Technology*.
- Moya, D., Aldas, C., Kaparaju, P., Geothermal energy: Power plant technology and direct heat applications, *Renewable and Sustainable Energy Reviews*, Volume 94, October 2018, Pages 889-901. <https://doi.org/10.1016/j.rser.2018.06.047>
- National Academies of Sciences, Engineering, and Medicine. 2019. *Negative Emissions Technologies and Reliable Sequestration: A Research Agenda*. Washington, DC: The National Academies Press. <https://doi.org/10.17226/25259>.
- National Energy Technology Laboratory. (2024). NETL Carbon Storage FAQs: Illustration of Pressure Effects on CO₂ (based upon image from CO₂CRC). Retrieved from <https://www.netl.doe.gov/carbon-management/carbon-storage/faqs/carbon-storage-faqs>
- National Energy Technology Laboratory (2015). Regional Carbon Sequestration Partnership (RCSP) <https://netl.doe.gov/carbon-management/carbon-storage/RCSP>
- National Energy Technology Laboratory (2016). U.S. Carbon Storage Atlas – Fifth Edition (Atlas V); <http://www.netl.doe.gov/research/coal/carbon-storage/natcarb-atlas>
- National Renewable Energy Laboratory. (2023). Annual Technology Baseline. <https://atb.nrel.gov/electricity/2023/geothermal>
- Ogland-Hand, J. D., Cairncross, E., Adams, B. M., Middleton, R. S. (2024). Nationwide Assessment of Sedimentary Basin Geothermal Power. In *Proceedings of the 49th Workshop on Geothermal Reservoir Engineering (SGP-TR-227)*. Stanford University, Stanford, California, February 12-14, 2024. Carbon Solutions, University of Illinois at Chicago.
- Oldenburg, C. M., Jordan, P. D., & Burton, E. (2017). Recommendations for geologic carbon sequestration in California: I. Siting criteria and monitoring approaches, II. example application case study. *Final report deliverable under ARB agreement No. 15ISD007*.
- Opportunity: BIL - Rare Earth Element Demonstration Facility. (DE-FOA-0002618). (2022). Morgantown, WV.
- Parker, N. (2004). Using Natural Gas Transmission Pipeline Costs to Estimate Hydrogen Pipeline Costs.
- Pollyea R.M., Fairley J.P. Implications of spatial reservoir uncertainty for CO₂ sequestration in the east snake river plain, idaho (USA). *Hydrogeology J.* 2012;20(4):689-699. <https://www.proquest.com/scholarly-journals/implications-spatial-reservoir-uncertainty-co2/docview/1016440050/se-2>. doi: <https://doi.org/10.1007/s10040-012-0847-1>.

Peacock, J.R., Earney, T.E., Mangan, M.T., Schermerhorn, W.D., Glen, J.M., Walters, M., Hartline, C., 2020, Geophysical characterization of the Northwest Geysers geothermal field, California, *Journal of Volcanology and Geothermal Research*, Volume 399, 2020, 106882, ISSN 0377-0273, <https://doi.org/10.1016/j.jvolgeores.2020.106882>

Reid, M. R. (2013). Tectonic stress and the spectra of seismic shear-wave splitting. *Journal of Geophysical Research: Solid Earth*, 118(5), 2155-2176.

Richter, A, 2020. *Industry points to stable supply of geothermal for California electricity market*. Think Geoenergy, August 25, 2020. <https://www.thinkgeoenergy.com/industry-points-to-stable-supply-of-geothermal-for-california-electricity-market/>

Rizzi, C., & Rizos, D. (2023). *Harnessing Earth's Heat: Applications of Geothermal Energy*. <https://www.pluginandplaytechcenter.com/resources/harnessing-earths-heat-applications-of-geothermal-energy/>

Roberts, B. J. "Geothermal Resource of the United States: Identified Hydrothermal Sites and Favorability of Deep Enhanced Geothermal Systems (EGS)." Golden, CO: National Renewable Energy Laboratory, February 22, 2018. <https://www.nrel.gov/gis/assets/images/geothermal-identified-hydrothermal-and-egs.jpg>.

Roberts-Ashby, T. L., Brennan, S. T., Buursink, M. L., Covault, J. A., Craddock, W. H., Drake, R. M., ... & Corum, M. D. (2014). *Geologic framework for the national assessment of carbon dioxide storage resources—US Gulf Coast (No. 2012-1024-H)*. US Geological Survey. Rose, A. W. (2010). *Geological storage of carbon dioxide in the Pennsylvania portion of the Appalachian Basin*. Pennsylvania Geological Survey.

Sabatino, F., Grimm, A., Gallucci, F., van Sint Annaland, M., Kramer, G. J., & Gazzani M. (2021). A comparative energy and costs assessment and optimization for direct air capture technologies. *Joule*, 8(5), 2047-2076.

Sandalow, D., R. Aines, J. Friedmann, P. Kelemen, C. McCormick, I. Power, B. Schmidt, and S. Wilson. (2021). *Carbon Mineralization Roadmap – Innovation for Cool Earth Forum (ICEF) Roadmap Project*. November 2021.

Sarkodie-Kyeremeh, Justice and Ampomah, William and Jiawei Tu, David and Czarnota, Robert, *Advances in CO2 Geological Storage: Estimation of CO2 Storage Efficiency Factors for the San Juan Basin Formations (November 25, 2022)*. Proceedings of the 16th Greenhouse Gas Control Technologies Conference (GHGT-16) 23-24 Oct 2022, Available at SSRN: <https://ssrn.com/abstract=4286058> or <http://dx.doi.org/10.2139/ssrn.4286058>

Schenk, C. J., Mercier, T. J., Tennyson, M. E., Woodall, C. A., Marra, K. R., Leathers-Miller, H. M., & Le, P. A. (2020). *Assessment of undiscovered gas resources of the Sacramento Basin Province in California, 2019 (No. 2020-3036)*. US Geological Survey.

Shi, X., Qian, Y., Yang, S., 2020 Fluctuation Analysis of a Complementary Wind–Solar Energy System and Integration for Large Scale Hydrogen Production *ACS Sustainable Chemistry & Engineering* 2020 8 (18), 7097-7110 DOI: 10.1021/acssuschemeng.0c01054

Simpson, R. W., & Richards, P. G. (1981). Seismicity and the tectonics of transform faulting. *Reviews of Geophysics*, 19(3), 525-548.

- Sorensen, J. A., S. A. Smith, A. A. Dobroskok, W. D. Peck, M. L. Belobraydic, J. J. Kringstad, and Z.-W. Zeng, 2009, Carbon dioxide storage potential of the Broom Creek Formation in North Dakota: A case study in site characterization for large-scale sequestration, *in* M. Grobe, J. C. Pashin, and R. L. Dodge, eds., Carbon dioxide sequestration in geological media—State of the science: AAPG Studies in Geology 59, p. 279–296.
- Stolaroff, J. K., Pang, S., Li, W., Kirkendall, W. G. (2021) Transport Cost for Carbon Removal Projects With Biomass and CO2 Storage. *Frontiers in Energy Research*, (9) 639943
- TechnoEconomic Sensitivity Tool (TEST). Project Interspace.
<https://geomap.projectinterspace.org/test/>
- Tester, Jefferson W., et al. (2006) "The future of geothermal energy: Impact of enhanced geothermal systems (EGS) on the United States in the 21st century." Massachusetts Institute of Technology.
- The Clean Air Task Force. (n.d.). CCS Map: Carbon Capture and Storage Projects in the United States. Retrieved from <https://www.catf.us/ccsmapus/>
- Tomarov, G.V., Shipkov, A.A., 2017, Modern geothermal power: Binary cycle geothermal power plants, *Energy Conservation, New and Renewable Energy Sources*, Volume 64, pages 243–250, <https://doi.org/10.1134/S0040601517040097>
- United States Department of Energy - Geothermal Technologies Office. "Geothermal Basics." (2020). <https://www.energy.gov/eere/geothermal/geothermal-basics>
- United States Environmental Protection Agency, 2018, Underground Injection Control (UIC) Program Class VI Implementation Manual for UIC Program Directors, https://www.epa.gov/sites/default/files/2018-01/documents/implementation_manual_508_010318.pdf
- United States Geological Survey. (2013). National Assessment of Geologic Carbon Dioxide Storage Resources— Summary Version 1.1. https://pubs.usgs.gov/fs/2013/3020/pdf/fs2013-3020_508.pdf
- United States Geological Survey. (2020.). Faults and Earthquakes. <https://www.usgs.gov/natural-hazards/earthquake-hazards/faults-and-earthquakes>
- U.S. Department of Energy. "Assessment of Nuclear Energy to Support Negative Emission Technologies." (2023).
- U.S. Department of Energy - Geothermal Technologies Office. "Geothermal Basics." (2020).
- U.S. Department of Energy. "Geothermal Technologies Program: 2020 Annual Report."
- U.S. Energy Information Administration. "Geothermal Explained."
- U.S. Geological Survey. (2020). "Volcano Hazards." Retrieved from <https://www.usgs.gov/natural-hazards/volcano-hazards>.
- Van Horn, A., Amaya, A, Higgins, B., Muir, J., Scherer, J., Pilko, R., Ross, M., 2020, New Opportunities and Applications for Closed-Loop Geothermal Energy Systems, *Geothermal Rising Conference Transactions*, Vol. 44. P. 1123-1143.
- White, D., Bachu, S., & Fox, D. (2013). Carbon Dioxide Storage in Geological Media: State of the Science. Alberta Energy Regulator (AER).
- Wisian, K., Bhattacharya, S., Richards, M., 2023, The Texas Geothermal Resource: Regions and

Geologies Ripe for Development, *The Future of Geothermal in Texas, Chapter 4*, <https://doi.org/10.26153/tsw/44071>

Wohletz, K., & Heiken, G. (1992). *Volcanology and geothermal energy*. University of California Press.

Wurzbacher, J. A., Gebald, C., Brunner, S., & Steinfeld, A. (2016). Heat and mass transfer of temperature–vacuum swing desorption for CO₂ capture from air. *Chemical Engineering Journal*, (283), 1329-1338.

Xia, T., McPherson, B., Esser, R., Jia, W., Moodie, N., Chu, S., Lee, S., 2019, Forecasting commercial-scale CO₂ storage capacity in deep saline reservoirs: Case study of Buzzard's bench, Central Utah, *Computers & Geosciences*, Volume 126, 2019, Pages 41-51, ISSN 0098-3004, <https://doi.org/10.1016/j.cageo.2018.12.006>.

Zakharova, N. V., D. S. Goldberg, E. C. Sullivan, M. M. Herron, and J. A. Grau (2012), Petrophysical and geochemical properties of Columbia River flood basalt: Implications for carbon sequestration, *Geochem. Geophys. Geosyst.*, 13, Q11001, doi:[10.1029/2012GC004305](https://doi.org/10.1029/2012GC004305).

Zarrouk, S. J., & Moon, H., 2014. Efficiency of geothermal power plants: A worldwide review. *Geothermics*, 51, 142-153. <https://doi.org/https://doi.org/10.1016/j.geothermics.2013.11.000>.

ZEP (Zero Emissions Platform). (2011). *The costs of CO₂ storage: post-demonstration CCS in the EU*, European Technology Platform for Zero Emission Fossil Fuel Power Plants, Brussels.

Zhang, Y., 2002, The age and accretion of the Earth, *Earth-Science Reviews* 59, p. 235-263

Acknowledgements

The Battelle team would like to thank Alexandra Smith and Mary Dhillon at Fervo Energy for their insight into key aspects of enhanced geothermal energy development and pathways toward integration with the burgeoning DAC industry. We would also like to thank Mark Cyffka, Valerie Wilson, and Bart Scherpbier of AirMyne, Inc. for their insight into DAC processes, heat and power applications within DAC facilities, DAC economics, and integration of geothermal energy and DAC. An extra thanks goes to Bart Scherpbier, who provided an excellent peer review of our capacity & cost model. Additionally, we would also like to thank Eric Stautberg for his insight into the potential for sedimentary geothermal on the Texas Gulf Coast, as well as thoughtful conversations around sedimentary geothermal in basins around the country.

Furthermore, we would also like to acknowledge the extremely high-quality work of the Project InnerSpace team and their partners in building and making public the GeoMap™ interactive spatial database and GeoMap™ TEST tool. Leveraging these tools and their outputs has significantly improved the quality of our work.

Finally, we'd like to thank Alex Krowka, Michael Moore, and the rest of the USEA team for their funding and thoughtful guidance throughout the course of this study.